Title

Chordin-Like 1 Suppresses Bone Morphogenetic Protein 4-Induced Breast Cancer Cell Migration and Invasion.



Journal

Molecular and Cellular Biology, 36(10)

Authors

Cyr-Depauw, Chanèle
Northey, Jason
Tabariès, Sébastien
et al.

Publication Date

2016-05-15

DOI

10.1128/MCB.00600-15

Peer reviewed

AMERICAN SOCIETY FOR MICROBIOLOGY | Molecular and Cellular Biology

# Chordin-Like 1 Suppresses Bone Morphogenetic Protein 4-Induced Breast Cancer Cell Migration and Invasion

Chanèle Cyr-Depauw,[a,b] Jason J. Northey,[a,b]* Sébastien Tabariès,[a,c] Matthew G. Annis,[a,c] Zhifeng Dong,[a,c] Sean Cory,[d] Michael Hallett,[d] Jonathan P. Rennhack,[e] Eran R. Andrechek,[e] Peter M. Siegel[a,b,c]

Goodman Cancer Research Centre[a] and Departments of Biochemistry[b] and Medicine,[c] McGill University, Montréal, Québec, Canada; McGill Centre for Bioinformatics, Montréal, Québec, Canada[d]; Department of Physiology, Michigan State University, East Lansing, Michigan, USA[e]

**ShcA is an important mediator of ErbB2- and transforming growth factor β (TGF-β)-induced breast cancer cell migration, invasion, and metastasis. We show that in the context of reduced ShcA levels, the bone morphogenetic protein (BMP) antagonist chordin-like 1 (Chrdl1) is upregulated in numerous breast cancer cells following TGF-β stimulation. BMPs have emerged as important modulators of breast cancer aggressiveness, and we have investigated the ability of Chrdl1 to block BMP-induced increases in breast cancer cell migration and invasion. Breast cancer-derived conditioned medium containing elevated concentrations of endogenous Chrdl1, as well as medium containing recombinant Chrdl1, suppresses BMP4-induced signaling in multiple breast cancer cell lines. Live-cell migration assays reveal that BMP4 induces breast cancer migration, which is effectively blocked by Chrdl1. We demonstrate that BMP4 also stimulated breast cancer cell invasion and matrix degradation, in part, through enhanced metalloproteinase 2 (MMP2) and MMP9 activity that is antagonized by Chrdl1. Finally, high Chrdl1 expression was associated with better clinical outcomes in patients with breast cancer. Together, our data reveal that Chrdl1 acts as a negative regulator of malignant breast cancer phenotypes through inhibition of BMP signaling.**

Breast cancer is a heterogeneous disease that can be subdivided into distinct molecular subtypes through the integration of gene expression and genomics data (1, 2). While ErbB2$^+$ breast cancers are considered a poor-prognosis subtype (3), other signaling pathways can further modulate their malignant phenotypes. The transforming growth factor β (TGF-β) family is a prominent example that has been shown to enhance the migratory, invasive, and metastatic abilities of ErbB2$^+$ breast cancer cells (4–7). We have previously demonstrated that the ShcA adaptor protein plays an important role, downstream of TGF-β and ErbB2 signaling pathways, in mediating these cellular responses (8, 9). Loss of ShcA expression in ErbB2-expressing cells significantly reduced tumor growth, which was the result of reduced proliferation, diminished endothelial cell recruitment, and elevated apoptosis (9). In the present study, through the use of microarray based transcriptional profiling, we identified elevated levels of chordin-like 1 (Chrdl1) in ErbB2$^+$ breast cancer cells following TGF-β stimulation; however, this upregulation of Chrdl1 occurs only in the context of diminished ShcA levels.

Bone morphogenetic proteins (BMPs) are secreted cytokines that belong to the TGF-β family of proteins, and their aberrant expression is observed in numerous cancers, including breast cancer (10). However, much like the TGF-β isoforms, there are conflicting reports on whether BMPs exert pro- or antitumorigenic effects on cancer cells (11, 12). In breast cancer, BMP4 has been shown to promote cancer cell migration and invasion (13–16). Similarly, BMP7 induces breast cancer cell proliferation, migration/invasion, and metastasis (17, 18). Interestingly, BMP4 and BMP7 are the most frequently and most highly expressed family members in breast cancer (10, 14).

Several factors influence BMP expression and activity. The BMP pathway can be negatively regulated by BMP antagonists, which are secreted proteins that bind BMP ligands and block their interactions with cognate cell surface receptors (19). A tight balance between BMP and BMP antagonist activity is required during development and normal tissue homeostasis in the adult. Disruption of this balance contributes to the progression of numerous diseases, including cancer (20). Chrdl1 is a secreted antagonist of BMP-mediated signaling via the Smad pathway, and it has previously been reported to predominantly inhibit BMP4-mediated signaling (21). While Chrdl1 function has been studied mainly in the context of development, little is known about its putative role in breast cancer.

In the current study, we demonstrated that, in the context of reduced ShcA signaling, Chrdl1 expression is upregulated in numerous breast cancer cells following TGF-β stimulation. Through a series of *in vitro* experiments, we demonstrated that Chrdl1 acts as an inhibitor of BMP4-induced migration and invasion. Moreover, Chrdl1 expression serves as a prognostic factor for better outcomes in patients with breast cancer.

## MATERIALS AND METHODS

**Generation of an inducible ShcA knockdown system in NMuMG-ErbB2 breast cancer cells.** Retrovirus harboring the reverse Tet transactivator (rtTA) was generated using 293 vesicular stomatitis virus (VSV)

**Received** 15 June 2015 **Returned for modification** 21 July 2015
**Accepted** 3 March 2016

**Accepted manuscript posted online** 14 March 2016

**Citation** Cyr-Depauw C, Northey JJ, Tabariès S, Annis MG, Dong Z, Cory S, Hallett M, Rennhack JP, Andrechek ER, Siegel PM. 2016. Chordin-like 1 suppresses bone morphogenetic protein 4-induced breast cancer cell migration and invasion. Mol Cell Biol 36:1509–1525. doi:10.1128/MCB.00600-15.

Address correspondence to Peter M. Siegel, peter.siegel@mcgill.ca.

* Present address: Jason J. Northey, Center for Bioengineering and Tissue Regeneration, Department of Surgery, University of California, San Francisco, San Francisco, California, USA.

C.C.-D. and J.J.N. contributed equally to this article.

packaging cells as previously described (22). NMuMG cells were transduced with virus and selected using 400 μg/ml of neomycin-G418 (Wisent) to generate a pooled cell population expressing the rtTA. Clonal populations were subsequently established and characterized for doxycycline inducibility using a tetracycline responsive element (TRE)-luciferase reporter construct (Clontech). Briefly, transient retroviral infections were performed with the TRE-luciferase reporter; individual clones were subsequently split into two pools and left untreated or treated with 2 μg/ml of doxycycline for 48 h. Cell lysates were prepared with luciferase assay cell lysis buffer from the Promega luciferase assay system (catalog number E1500). Whole-cell protein lysates (20 μg) from each clonal cell population (treated and untreated) were aliquoted into 96-well plates, luciferase assay reagent added to each well, and luciferase activity measured with a BMG FLUOstar Omega plate reader (Imgen Technologies). Luminescence readings were normalized to protein concentrations determined from the cell lysates, and induced luciferase expression was determined by plotting normalized luminescence values with and without doxycycline treatment.

Populations that exhibited a 13-fold or greater induction in luciferase activity following doxycycline treatment were selected and subsequently transduced with the TMP vector containing microRNA-designed RNA interference (RNAi) sequences (shRNAmirs) targeting the ShcA or luciferase gene. Clones that exhibited an efficient knockdown of ShcA in response to doxycycline treatment (2 μg/ml, 72 h) were then transduced with virus containing a NeuNT cDNA (rat ortholog of activated ErbB2; here denoted ErbB2). NMuMG clones bearing luciferase gene control short hairpin RNAs (shRNAs), which showed no decrease in ShcA levels following doxycycline treatment, were also transduced with activated ErbB2.

**DNA constructs and RNAi sequences.** We utilized microRNA-designed sequences (shRNAmirs) to target either the 3′ untranslated region (3′UTR) of the ShcA gene or luciferase gene transcripts as a control, as previously described (9). The shRNAmirs were expressed under the control of a doxycycline-inducible promoter using the retroviral TMP vector system (catalog number EAV4678; Open Biosystems).

**Cell lines and cell culture.** NMuMG-derived cell populations and explants (8)were treated with 2 μg/ml doxycycline for 48, 72, or 96 h prior to experimentation, as required. The MDA-MB-231, BT549, and HCC1954 cell lines were purchased from the American Type Culture Collection (Manassas, VA), and NIC cell populations were derived from mammary tumors that formed in mouse mammary tumor virus (MMTV)/NIC mice (22). Retroviruses were generated in 293VSV packaging cells according to the manufacturer's instructions (Clontech). NMuMG-ErbB2 (8), NIC (22), and human breast cancer (MDA-MB-231, BT549, and HCC1954) cell lines were cultured as previously described (23–25).

**siRNA transfection.** Expression of the endogenous ShcA gene was transiently diminished in NICs and the MDA-MB-231 and BT549 breast cancer cell lines by expression of small interfering RNAs (siRNAs) directed against the 3′UTR of the ShcA gene. A mixture of 2 dicer substrate duplex siRNAs (5′-AGCAGACAGUUGCGUGAUCCGGAAC-3′ and 5′-CAGCCUGAAUAUGGUGGCGCAC-3′) targeting the mouse ShcA gene was used for the transfection of mouse NIC cells, and a mixture of 3 dicer substrate duplex siRNAs (5′-AGAUGCCCUCCAAUCCUUUCCACCC-3′, 5′-CCUAU GUACUCUACGCCAAAGUGCA-3′, and 5′-UGAGACU AUAAAGCAGUAGACAATC-3′) was used for targeting the human ShcA gene in MDA-MB-231 and BT549 cells. The breast cancer cells were also transfected with a scrambled dicer substrate duplex siRNA as a control. siRNAs were used at a final concentration of 60 nM per transfection (20 nM for each individual ShcA siRNA). INTERFERin transfection reagent (catalog number 409-50; Polyplus Transfection) was used to perform all transfections according to the manufacturer's protocol. Cells were serially transfected 3 times: once following cell plating, again 6 h later, and a final time at 18 h after the second transfection. Prior to each transfection, cells were lightly trypsinized to enhance transfection efficiency. Six hours following the last transfection, cells were treated with 2 ng/ml of TGF-β1 (catalog number HZ-1011; Humanzyme, Chicago, IL) for 24 h (NICs and MDA-MB-231) or 48 h (BT549), and conditioned media and whole-cell lysates were collected and subjected to enzyme-linked immunosorbent assay (ELISA) and immunoblotting as described below.

**Mammary tumor growth.** Two clonal populations expressing either the ShcA or luciferase gene-targeting shRNAmirs were injected into the mammary fat pads of athymic mice to generate tumorigenic populations. NMuMG-ErbB2 breast cancer cells ($1 \times 10^6$) were injected into the inguinal mammary fat pads in a 50-μl volume of phosphate-buffered saline (PBS) and Matrigel (50:50) (catalog number 356234; BD Biosciences), and mice were not exposed to doxycycline, ensuring that the shRNAs were not expressed. Tumor growth was monitored every 2 weeks by caliper measurement for 6 weeks, and tumor volumes were calculated using the formula $\pi LW^2/6$, where $L$ is the length and $W$ is the width of the mammary tumor. Tumors were excised at a defined tumor volume, and explant populations were generated by mincing the tumor tissue and then incubating for 20 min at 37°C in 0.05% trypsin (Wisent). Explant populations were plated in fresh medium containing puromycin, hygromycin, and neomycin-G418 to maintain expression of the shRNAmir, ErbB2, and the rtTA, respectively. Three individual tumor explants of each ErbB2/rtTA population, expressing either the ShcA or luciferase gene control shRNAmirs, were pooled to reduce clonal variation.

To assess primary tumor growth of the ErbB2/rtTA/ShcA-KD and ErbB2/rtTA/Luc-KD cells, $1 \times 10^5$ cells from each cell population were injected into the mammary fat pads of female SCID/beige mice. When tumor volumes reached a range of 150 to 200 $mm^3$, doxycycline treatment was initiated by adding doxycycline to the drinking water (containing 10% sucrose) at a final concentration of 2 mg/ml. Mammary tumors were harvested at 6 weeks postinjection, and portions were flash frozen in liquid nitrogen or fixed and embedded in paraffin. Mice were housed in facilities managed by the McGill University Animal Resources Centre, and all animal experiments were conducted under a McGill University-approved animal use protocol in accordance with guidelines established by the Canadian Council on Animal Care.

**RNA isolation, amplification, labeling, and hybridization to Agilent microarrays.** Basic procedures for the manipulation of RNA samples were previously described (26), and a single round of amplification was performed for all RNA samples prior to labeling and hybridization. NMuMG-ErbB2/rtTA/ShcA-KD and NMuMG-ErbB2/rtTA/Luc-KD cells were plated into 10-cm tissue culture dishes and treated with or without 2 μg/ml doxycycline for 96 h. These breast cancer cells were left untreated or stimulated for 3 or 24 h with TGF-β, and total RNA was extracted using QIAshredder and RNeasy spin columns (Qiagen). Gene expression analyses were performed on duplicate samples of the NMuMG-ErbB2/rtTA/Shc-KD and NMuMG-ErbB2/rtTA/Luc-KD populations (technical replicates). Purified RNA was subjected to reverse transcription, amplification, and labeling protocols as previously described (26). Labeled RNA was hybridized to 4x44K version2 whole mouse genome microarray gene expression chips (Agilent Technologies) for 17 h at 60°C. The microarray chips were then washed, dried with gaseous $N_2$, and immediately scanned using a DNA microarray scanner (model G2565BA; Agilent Technologies).

**Gene expression analysis.** Raw data were normalized using the normexp background correction and quantile between array normalization methods. Differential expression was performed using a $t$ test with false-discovery-rate (FDR) correction. Using a fold change (FC) of $>1.5$ and an FDR of $<0.05$, we identified 125 genes that were differentially expressed in response to TGF-β (3 h or 24 h) and that were dependent on ShcA expression. A subset of these genes were included in the heat map, of which the Chrdl1 gene was the gene whose increase in expression by TGF-β was most dependent on ShcA loss. Gene ontology (GO) analysis was performed by examining GO categories for overrepresentation in the set of differentially expressed genes (uncorrected $P$ value of less than 0.05) using a hypergeometric test. All microarray analysis was performed using R/bioconductor (27).

**Total RNA extraction and RT-qPCR.** NMuMG-ErbB2 doxycycline-inducible ShcA knockdown cells were treated with 2 μg/ml doxycycline for 96 h or not treated and left unstimulated or stimulated with TGF-β (2 ng/ml) for 3 or 24 h. Cells were then grown to 70 to 80% confluence and subjected to RNA isolation using QIAshredder columns and the RNeasy minikit (Qiagen) according to the manufacturer's protocol. Total RNA was quantified and subjected to reverse transcription-quantitative PCR (RT-qPCR) as previously described (28). Each experiment was performed in triplicate and normalized to mouse GAPDH (glyceraldehyde-3-phosphate dehydrogenase) gene expression. The primer sequences used for *Chrdl1*, the metalloproteinase 2 gene (*Mmp2*), *Mmp9*, *Mmp14*, and *Gapdh* were as follows: Chrdl1 forward, 5′-GTGATTCCCCTGCTAGATGA-3′; Chrdl1 reverse, 5′-TCCCACAGCACTTTAGGAAG-3′; *Mmp2* forward, 5′-GAAGTTCCCCGGCGATGTC-3′; *Mmp2* reverse, 5′-TTCTGGTCAAGGTCACCTGTC-3′; *Mmp9* forward, 5′-CAATCCTTGCAATGTGGATG-3′; *Mmp9* reverse, 5′-AGTAAGGAAGGGGCCCTGTA-3′; *Mmp14* forward, 5′-CAGTATGGCTACCTACCTCCAG-3′; *Mmp14* reverse, 5′-GCCTTGCCTGTCACTTGTAAA-3′; *Gapdh* forward, 5′-CAAGTATGATGACATCAAGAAGGTGG-3′; *Gapdh* reverse, 5′-GGAAGAGTGGGAGTTGCTGTTG-3′.

**Conditioned medium and protein extraction.** To assess Chrdl1 expression, NMuMG-ErbB2/rtTA/ShcA-KD cells were plated at 30 to 40% confluence, pretreated in the presence or absence of doxycycline for 48 h, and costimulated with TGF-β (2 ng/ml) or not costimulated for the last 3 or 24 h. Cell lysates and conditioned medium were collected to perform ELISAs.

To evaluate the effects of conditioned medium harvested from NMuMG-ErbB2/rtTA/ShcA-KD cells on BMP4-induced signaling, these cells were first cultured to 30 to 40% confluence. The following day, cells were treated with or without doxycycline for 72 h in conjunction with TGF-β stimulation (2 ng/ml) for 24 h. Subsequently, conditioned medium was harvested and added to a fresh culture of NMuMG-ErbB2/rtTA/ShcA-KD cells that had been serum starved overnight. The same cultures were then stimulated with BMP4 (2.5 ng/ml) (catalog number 315-27; PeproTech) or not stimulated. Thirty minutes later, conditioned medium and cell lysates were harvested to perform ELISA and immunoblotting.

To directly examine the effects of Chrdl1, breast cancer cells were treated with human recombinant Chrdl1 (rChrdl1) (catalog number 1808-NR/CF; R&D Systems). Briefly, NMuMG-ErbB2, BT549, and HCC1954 cells were cultured to 30 to 40% confluence and then serum starved overnight. Subsequently, breast cancer cells were stimulated with BMP4 (2.5 ng/ml) or TGF-β (2 ng/ml) or not stimulated in the presence or absence of increasing rChrdl1 concentrations for 30 min. Cell lysates were collected and subjected to immunoblotting. Cells stimulated with BMP4 (2.5 ng/ml) or not stimulated in the presence or absence of rChrdl1 (100 ng/ml) were subjected to Li-Cor quantitative immunoblot analysis.

All cells were washed with 1× PBS and lysed in TNE lysis buffer (50 mM Tris-HCl [pH 8.0], 150 mM NaCl, 1% NP-40, 2 mM EDTA [pH 8.0], 0.1 mM sodium orthovanadate, 10 μg/ml aprotinin, 10 μg/ml leupeptin, 10 mM NaF, 2.5 mM sodium pyrophosphate, 1 mM β-glycerol phosphate). Protein concentrations were measured by Bradford assay.

**ELISAs.** For each cell population and experimental condition, conditioned medium was collected and cell lysates were prepared in TNE lysis buffer. Cell lysates were quantified by Bradford assay, and ELISAs were performed to obtain quantitative measurements of secreted Chrdl1 according to the manufacturer's protocol. Secreted Chrdl1 concentrations were normalized to protein concentrations measured from whole-cell protein lysates. All incubations and washes were performed as suggested by the manufacturer. Luminescence readings of each sample were measured using an automated Omega plate reader at a wavelength of 450 nm.

**Immunoblot analysis.** rChrdl1 was titrated to identify the concentration that maximally impaired BMP4 and BMP7 (50 ng/ml) (catalog number 120-03; Peprotech). Total protein (30 to 40 μg) was separated by 7.5% SDS-polyacrylamide gel electrophoresis (PAGE) and resolved proteins transferred onto polyvinylidene difluoride (PVDF) membranes. Membranes were blocked for 1 h with 5% milk solution, except for membranes used to detect pSmad1/5/8, total Smad2/3, and ShcA, for which 5% bovine serum albumin (BSA) solution was used as the blocking agent. Membranes were washed with 1× Tris-buffered saline (TBS)–1% Tween 20 and incubated overnight at 4°C using the following antibodies, as indicated: ShcA (1:1,000 dilution) (catalog number 610081; BD Biosciences), FLAG (M2) (1:1,000 dilution) (catalog number F1804; Sigma), ErbB2/Neu (C-18) (1:1,000 dilution) (catalog number sc-284-G; Santa Cruz), phospho-Smad 1/5/8 (1:1,000 dilution) (catalog number 9511; Cell Signaling), phospho-Smad1/8 (1:1,000 dilution) (catalog number 562508; BD Biosciences), Smad1 (1:1,000 dilution) (catalog number 38-5400; Invitrogen), Smad2/3 (1:1,000 dilution) (catalog number 610842; BD Biosciences), phospho-Smad2 (Ser465/467) (1:1,000 dilution) (catalog number 3101; Cell Signaling), and α-tubulin (1:5,000 dilution) (catalog number T9026; Sigma). Membranes were washed 3 times with 1× TBS–1% Tween 20 and incubated with appropriate horseradish peroxidase (HRP)-conjugated secondary antibodies (1:10,000 dilution) for 1 h. The membranes were washed 3 times with 1× TBS–1% Tween 20 and visualized with an enhanced chemiluminescence system.

**Quantitative immunoblot analysis.** For quantification of phospho-Smad1/8 immunoblots using the Odyssey IR imager, immunoblotting was performed as described above with the exception that the membrane was blocked in Odyssey blocking buffer (Li-Cor) for 1 h. Membranes were incubated at 4°C overnight with phospho-Smad1/8 antibodies (1:1,000 dilution) (catalog number 562508; BD Biosciences) and Smad1 antibodies (1:1,000 dilution) (catalog number 38-5400; Invitrogen), which were diluted in Odyssey blocking buffer containing 0.2% Tween 20. Membranes were washed and subsequently incubated for 45 min in blocking buffer containing Tween 20 (0.3%, vol/vol), 0.02% SDS, 1 mg/ml anti-rat IgG conjugated to IR dye 680 (Li-Cor), and 1 mg/ml anti-rabbit IgG conjugated to IR dye 800 (Li-Cor) and protected from light. Membranes were scanned in the 500-nm channel using the Odyssey IR imager, and phospho-Smad1/8 and Smad1 protein levels were quantified using the Image Studio Lite software package.

**Immunohistochemistry.** Tissue fixation, immunohistochemical (IHC) staining, and quantification of positive staining were carried out as previously described (9). Immunohistochemical staining was performed on NMuMG-ErbB2/ShcA$^{high}$ and NMuMG-ErbB2/ShcA$^{low}$ mammary tumors that have been described previously (9). Mammary tumors were fixed overnight in 4% paraformaldehyde. Primary antibodies were used to detect ShcA (1:100 dilution) (catalog number ab24787; Abcam) and Chrdl1 (1:100 dilution) (catalog number ab103369; Abcam) in conjunction with the appropriate biotin-SP-conjugated anti-IgG secondary antibodies (Jackson Laboratories, Bar Harbor, ME). Sections were developed with 3-3-diaminobenzidine-tetrahydrochloride and counterstained with hematoxylin.

**Cell-tracking migration assays.** NMuMG-ErbB2 or BT549 cells ($6 \times 10^3$) were plated in 24-well plates previously coated with 4.5 μg/cm$^2$ of fibronectin and allowed to adhere for 45 min at 37°C prior to cell imaging. Cell tracking was performed using conventional phase-contrast microscopy (Zeiss Axiovert 200M), and cells were imaged using a Zeiss AxioCam monochrome (3,900 by 3,900 pixels) camera once every 10 min for 28 h. After 5 h, cells were treated with or without TGF-β (2 ng/ml) or BMP4 (2.5 ng/ml) in the presence or absence of human recombinant Chrdl1 (100 ng/ml). After data acquisition, 10 to 20 cells were tracked manually using MetaXpress for each time point. The velocity in micrometers per hour was calculated for each cell, as well as the mean velocity and standard deviation.

**Invasion assays.** The BT549 and HCC1954 cell lines were used for the evaluation of cell invasion using Boyden chamber assays. Cells were pretreated with or without BMP4 (2.5 ng/ml) and in the presence or absence of human recombinant Chrdl1 (100 ng/ml) for 24 h. BT549 ($8.5 \times 10^4$) and HCC1954 ($4 \times 10^4$) cells were subsequently trypsinized, resuspended in serum-free medium, and plated onto 6% Matrigel that was overlaid on

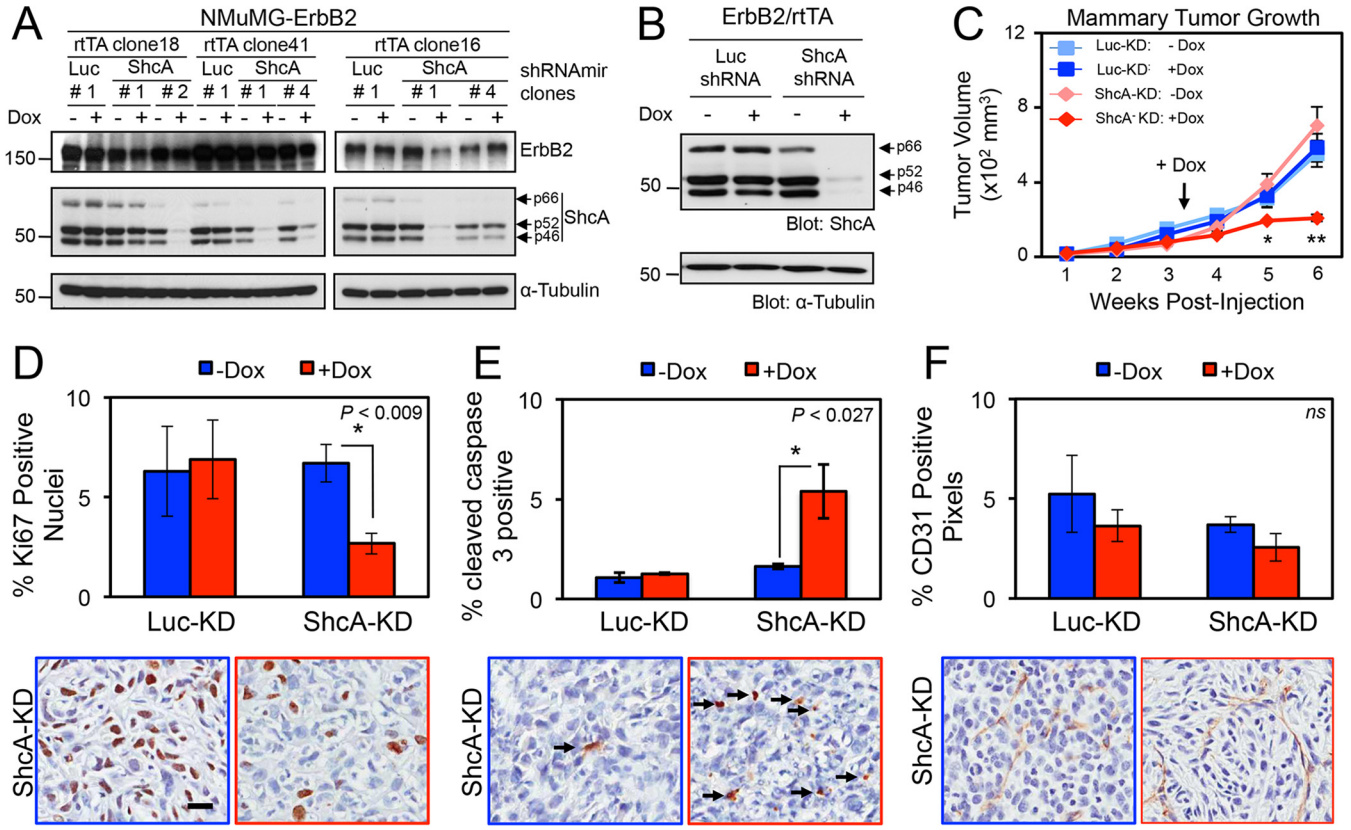


**FIG 1** Inducible reduction of ShcA expression impairs mammary tumor growth. (A) A doxycycline-inducible system for diminishing ShcA expression. NMuMG-ErbB2/rtTA cells harboring ShcA or luciferase control shRNA sequences were left untreated or treated with doxycycline (Dox). Whole-cell protein lysates were subjected to immunoblot analysis with antibodies specific for ErbB2/Neu, ShcA, and α-tubulin. (B) ErbB2/rtTA-expressing tumor explant populations harboring shRNAs targeting ShcA (ShcA shRNA) or luciferase (Luc shRNA) were stimulated with doxycycline (+Dox) or not stimulated (−Dox) for 48 h. Immunoblot analysis was performed on whole-cell lysates with antibodies against ShcA and α-tubulin. (C) Mammary tumor growth of ErbB2/rtTA/ShcA-KD and ErbB2/rtTA/Luc-KD cells ($n = 20$ for each cell line). When tumors reached volumes between 100 and 150 $mm^3$ (3 weeks postinjection), mice from each cohort were left untreated (−Dox; $n = 10$) or received doxycycline treatment (+Dox; $n = 10$) through their drinking water. *, $P < 0.050$; **, $P < 0.002$. (D to F) Immunohistochemical staining was performed on paraffin-embedded mammary tumor sections for markers of proliferation (Ki67) (*, $P < 0.009$) (D), apoptosis (cleaved caspase-3) (*, $P < 0.027$) (E), and endothelial cell recruitment (CD31) (F). Representative images are shown. Arrows included in the cleaved-caspase-3 IHC panels indicate apoptotic cells. Scale bar in panel D, 50 μm (applies to all panels).

the top chamber of transwell inserts (8.0-μm pore size) (catalog number 353097; Falcon). The presence or absence of BMP4 and Chrdl1 in the top chamber of each transwell is indicated. In the lower chamber, 1 ml of standard cell medium containing 10% fetal bovine serum (FBS) was added, and the cells were allowed to invade through the membrane for 24 h at 37°C. Quantification of invading cells was performed as previously described (9). The data represent the averages from three (BT549) or four (HCC1954) independent experiments performed in triplicate.

**Fluorescent gelatin degradation assay.** Glass coverslips were coated with 0.1 mg/ml poly-D-lysine for 20 min at room temperature. Subsequently, glass coverslips were washed 3 times with PBS and incubated at room temperature with glutaraldehyde for 20 min. After washing 3 times with PBS, glass coverslips were incubated at 37°C for 1 h in gelatin matrix consisting of diluted cross-linked-fluorophore (fluorescein isothiocyanate [FITC])-conjugated gelatin (catalog number G13187; Gibco/Invitrogen) in 0.1% unlabeled gelatin (1:50) and fibronectin (4.5 $\mu g/cm^2$). Glass coverslips were washed 3 times with PBS, incubated at room temperature with 10% $NaBH_4$ for 1 min, washed again in PBS, incubated at room temperature with 70% ethanol for 20 min, and then given a final PBS wash. The fluorescent-gelatin-coated coverslips were quenched in Dulbecco modified Eagle medium (DMEM) containing 10% FBS for 1 h at 37°C prior to plating the indicated breast cancer cells. NMuMG-ErbB2 and BT549 cells pretreated with or without BMP4 (2.5 ng/ml), in the presence or absence of human recombinant Chrdl1 (100 ng/ml), for 24 h were plated onto the fluorescent-gelatin-coated coverslips in 24-well plates ($3 \times 10^4$ NMuMG-ErbB2 cells and $4.5 \times 10^4$ BT549 cells). Cells were stimulated with BMP4 (2.5 ng/ml) or not stimulated in the presence or absence of Chrdl1 (100 ng/ml) for an additional 24 h at 37°C. Breast cancer cells were fixed for 20 min with 2% paraformaldehyde in PBS, permeabilized with PBS containing 0.2% Triton X-100 for 10 min, and then washed 3 times with 100 mM glycine in PBS. To block the cells, a 30-min incubation in PBS containing 0.2% Triton X-100, 0.05% Tween 20, and 2% bovine serum albumin was performed. Images were captured using an LSM510 confocal microscope at a magnification of ×100. To quantitate the degree of cell-mediated degradation, a total of 20 images per experiment were captured and analyzed using CellTracker. The mean from 2 independent experiments was calculated for each condition.

**Gel zymography.** NMuMG-ErbB2 and BT549 cells were plated to 40% confluence and stimulated with BMP4 (2.5 ng/ml) or not stimulated in the presence or absence of human recombinant Chrdl1 (100 ng/ml). After a 24-h incubation at 37°C, conditioned medium was harvested and separated by 7.5% SDS-PAGE with 0.1% gelatin. Subsequently, gels were washed 3 times with 2.5% Triton X-100 and incubated in reaction solution (50 mM Tris-HCl [pH 7.4], 5 mM $CaCl_2$, 200 mM NaCl) for 24 h at 37°C under gentle agitation. The reaction was stopped and the gels stained with Coomassie blue solution (0.25% Coomassie blue, 50% methanol,

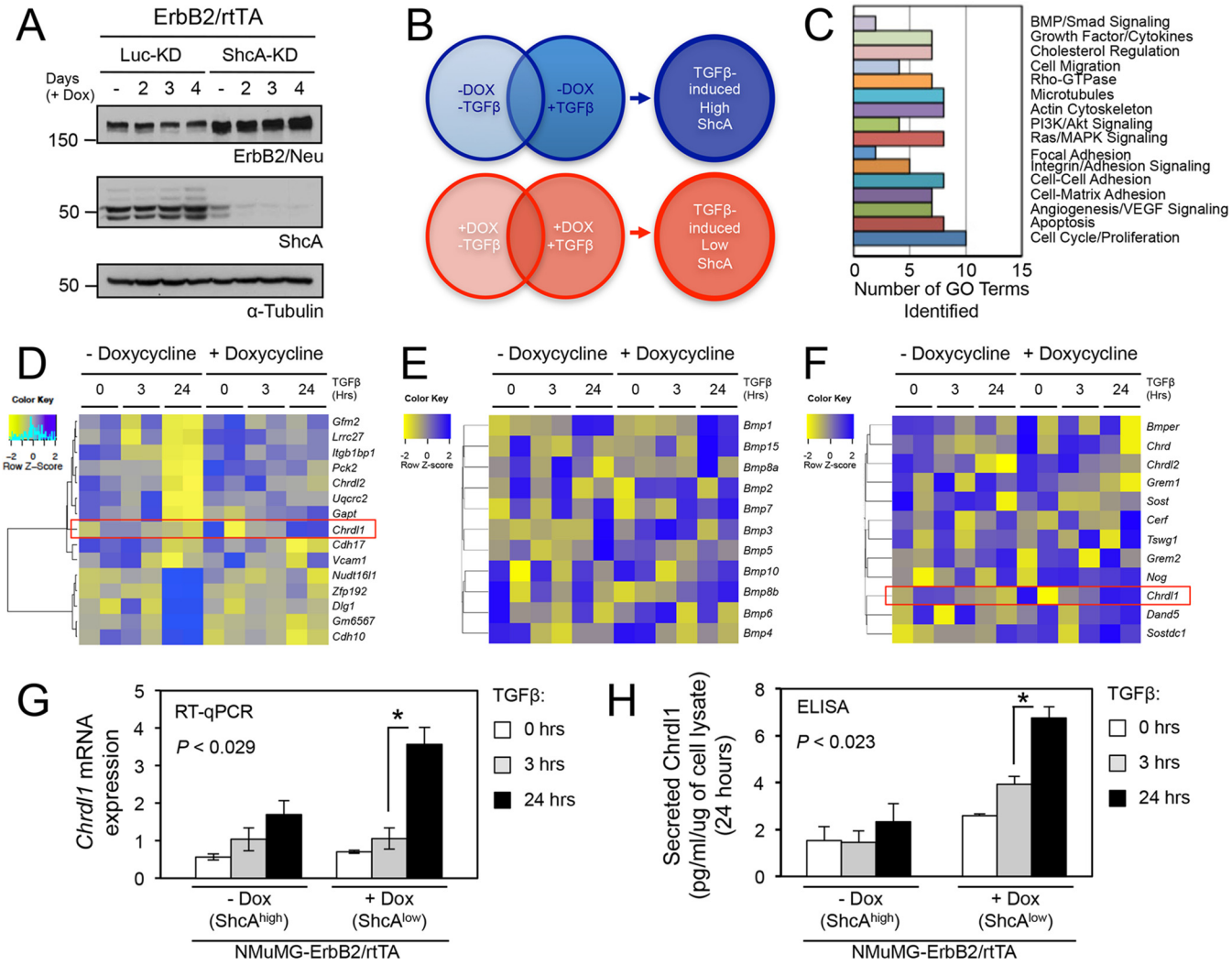


**FIG 2** TGF-β-induced, ShcA-dependent gene expression profiling in ErbB2-expressing breast cancer cells identifies Chrdl1. (A) Immunoblot analysis of NMuMG-ErbB2/rtTA cells following doxycycline treatment for the indicated times using antibodies against ShcA, ErbB2, and α-tubulin. (B) Schematic of experimental design. (C) Gene ontology analysis of differentially expressed genes. (D) Gene expression heat maps of the most differentially expressed genes in ErbB2-expressing breast cancer cells following TGF-β treatment (2.5 ng/ml) (3 or 24 h) in the context of high (−Dox) or low (+Dox) ShcA levels. A yellow to blue gradient represents low to high gene expression levels. The red box highlights Chrdl1 Agilent gene expression data. (E and F) TGF-β-induced, ShcA-dependent gene expression of BMP family members or BMP antagonists in ErbB2-expressing breast cancer cells. Gene expression heat maps of BMP genes (E) or BMP antagonist genes (F) in breast cancer cells following TGF-β treatment (3 or 24 h) in the context of high (−Dox) or low (+Dox) ShcA levels are shown. A yellow to blue gradient represents low to high gene expression levels. The red box highlights Chrdl1 Agilent gene expression data. (G) RT-qPCR analysis of *Chrdl1* mRNA expression levels following TGF-β stimulation in the presence or absence of ShcA. *, $P < 0.029$. (H) Chrdl1 secreted protein expression levels were monitored by ELISA using conditioned medium harvested under the conditions described for panel G. Secreted Chrdl1 concentrations were normalized to protein concentrations measured in whole-cell protein lysates. *, $P < 0.023$.

10% acetic acid) for 30 min prior to being destained for 15 min (50% methanol, 10% acetic acid). Bands were visualized using a GelDoc-It Imager (UVP) and quantified using the Image Studio Lite software package.

**Clinical analysis of *Chrdl1* expression.** To assess associations between *Chrdl1* expression and overall survival (OS), disease-free survival (DFS), and distant metastasis-free survival (DMFS) of breast cancer patients or OS of lung, ovarian, and gastric cancer patients, we used the kmplot.com data set (database version 2014) (29–31). *Chrdl1* levels were queried through the use of Affymetrix probe ID 209763_at. Patients were split into high- and low-expressing groups based upon median *Chrdl1* expression. Biased arrays were excluded from the analysis. Additional settings used for the analysis of the kmplot.com data set were as follows: follow-up threshold, all; probe set options, only JetSet best probe set. No other filters were applied to the patient population before Kaplan-Meier analysis.

**Statistical analysis.** Statistical significance values (*P* values) for RT-qPCR, ELISA data, and migration and invasion experiments were obtained by performing a two-sample unequal-variance Student *t* test.

## RESULTS

**Generation of a doxycycline-inducible system for reducing ShcA expression.** We have previously shown that stable shRNA-mediated silencing of ShcA expression impairs the growth and metastasis of ErbB2-expressing breast tumors (9). However, this approach did not permit investigation of the temporal require-

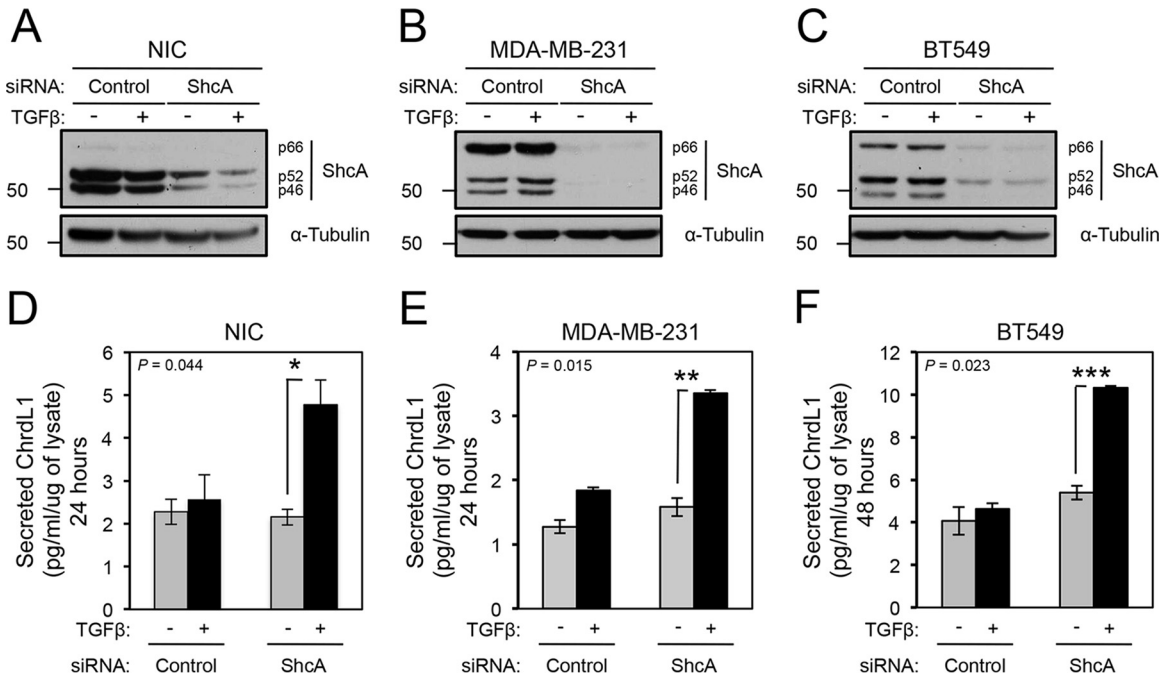


**FIG 3** Chrdl1 expression is elevated following TGF-β stimulation of HER2$^+$ and basal breast cancer cells in the context of reduced ShcA levels. (A to C) Immunoblot analysis of ShcA expression was performed in NIC (A), MDA-MB-231 (B), and BT549 (C) breast cancer cells transfected with scrambled or ShcA-specific siRNAs. Cells were stimulated with TGF-β (+) or not stimulated (−) for 24 (NIC and MDA-MB-231) or 48 h (BT549). In all cases, α-tubulin was used as a loading control. (D to F) ELISAs were performed to detect secreted Chrdl1 levels in the conditioned media of NIC (D), MDA-MB-231 (E), and BT549 (F) breast cancer cells. Secreted Chrdl1 concentrations were normalized to protein concentrations from whole-cell protein lysates. *, $P = 0.044$; **, $P = 0.015$; ***, $P = 0.023$.

ment for ShcA during tumor growth and metastasis. To circumvent this limitation, we generated a doxycycline-inducible ShcA knockdown system. The same shRNAmir sequence used for a stable knockdown of ShcA (9) was cloned and expressed in a modified LMP vector, termed TMP, which contains a Tet-responsive element in the promoter (32). NMuMG cells were engineered to express the reverse Tet transactivator (rtTA), an activated form of ErbB2 (NeuNT), and shRNAmir sequences targeting the ShcA or luciferase gene as a negative control (Fig. 1A).

To overcome undesired clonal effects, two of the clonal populations from the ErbB2/rtTA/Shc-KD- and ErbB2/rtTA/Luc-KD-expressing cell lines (clone 18 and clone 16) were injected into the mammary fat pads of athymic mice to facilitate *in vivo* selection of tumorigenic populations. Mice were not treated with doxycycline to ensure that tumor growth was not affected by diminished ShcA expression. Mammary tumors were excised and established for *in vitro* culture, and three independent tumor explant populations were pooled to generate ErbB2/rtTA/Shc-KD and ErbB2/rtTA/Luc-KD NMuMG populations.

**Inducible silencing of ShcA expression impairs ErbB2-mediated tumorigenesis.** Immunoblot analysis of ErbB2/rtTA/Shc-KD cells revealed an efficient loss of ShcA expression following doxycycline treatment (Fig. 1B). Following mammary fat pad injection of these cells, the resulting tumors were allowed to grow to a volume of 150 to 200 mm$^3$ before the addition of doxycycline. The growth of ErbB2/rtTA/Shc-KD mammary tumors in doxycycline-treated mice was markedly impaired compared to their growth in the absence of doxycycline (Fig. 1C). Importantly, the growth of ErbB2/rtTA/Shc-KD tumors in untreated mice (−Dox) paralleled the growth of ErbB2/rtTA/Luc-KD tumors in mice that were untreated or treated with doxycycline (+Dox) (Fig. 1C). To ascertain the cause of delayed tumor outgrowth resulting from induced loss of ShcA expression, we examined tumor tissue sections by immunohistochemical staining for markers of proliferation (Ki67) (Fig. 1D), apoptosis (cleaved caspase-3) (Fig. 1E), and endothelial cell recruitment (CD31) (Fig. 1F). A significant ~1.8-fold decrease in proliferating cells and an ~3.3-fold increase in apoptotic cells were observed in tumors with reduced ShcA expression following doxycycline treatment. Interestingly, there was no significant difference in endothelial cell recruitment in ErbB2/rtTA/Shc-KD tumors from doxycycline-treated mice versus nontreated controls. These data argue that loss of ShcA expression in established mammary tumors still results in significantly impaired tumor growth.

**Identification of TGF-β-regulated, ShcA-dependent gene expression changes in ErbB2-expressing breast cancer cells.** To identify genes regulated by TGF-β signaling and differentially expressed specifically in context of high versus low ShcA levels, gene expression profiling was performed using NMuMG-ErbB2/rtTA/ShcA-KD cells. These cells were treated with or without doxycycline for 72 h to achieve cultures with both high (−Dox) and low (+Dox) ShcA expression (Fig. 2A). NMuMG-ErbB2/rtTA/ShcA-KD cells were treated with or without doxycycline and subsequently left untreated or stimulated with TGF-β for 3 or 24 h (Fig. 2B). Total RNA from each of these conditions was extracted, labeled, and hybridized to Agilent microarray chips. Gene expression analysis identified a total of 125 genes, out of approximately 2,900 genes, that were differentially expressed in response to

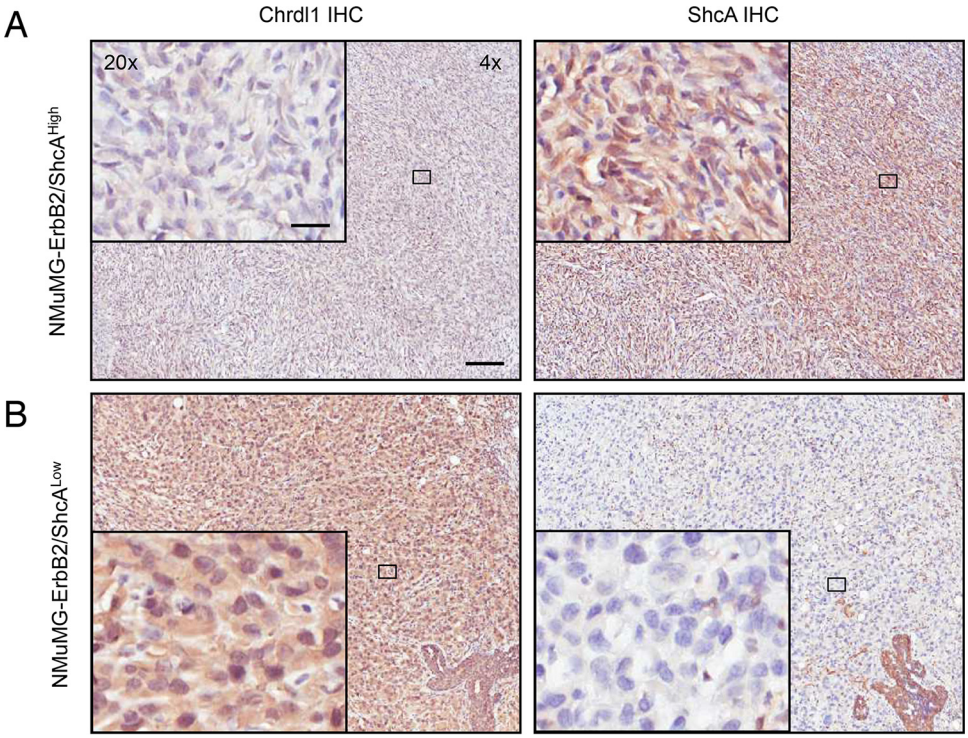


**FIG 4** Stable reduction of ShcA levels increases Chrdl1 expression within ErbB2-expressing mammary tumors *in vivo*. Representative images of ErbB2/ShcA$^{high}$ (A) and ErbB2/ShcA$^{low}$ (B) mouse mammary tumors following immunohistochemical (IHC) staining with antibodies against ShcA or Chrdl1 are shown. Scale bar in ×4 panel, 100 μm (applies to all panels). Scale bar in ×20 inset, 20 μm (applies to all panels).

TGF-β in the context of acute ShcA loss. To categorize these genes according to biological function, a gene ontology (GO) analysis approach was performed. A list of categories was constructed, and the numbers of significant GO terms that fell within these categories is shown in Fig. 2C. A heat map depicting some of the genes most differentially expressed in response to TGF-β stimulation in a ShcA-dependent manner was generated (Fig. 2D).

**Reduced ShcA signaling results in upregulation of Chrdl1 in breast cancer cells following TGF-β stimulation.** BMPs can promote breast cancer progression, and both BMP4 and BMP7 are highly expressed in breast cancer cell lines and primary breast tumors (10). Furthermore, BMP4 was reported to be a potent inducer of breast cancer cell growth and invasion (14). Chrdl1, which is known to inhibit BMP activity by directly binding to these ligands in the extracellular space (21, 33, 34), showed significantly higher gene expression levels in the context of diminished ShcA levels following 24 h of TGF-β stimulation (Fig. 2D). To interrogate whether the observed TGF-β-mediated upregulation of *Chrdl1*, in the context of reduced ShcA expression, was unique, we examined the expression of the known BMP family members and BMP antagonists for which probes were available in the Agilent gene expression arrays. The majority of BMPs exhibited the same expression profiles following TGF-β treatment in cells with normal versus reduced ShcA levels. The one exception was *Bmp15* gene expression, which was specifically elevated following 24 h of TGF-β stimulation in breast cancer cells with reduced ShcA expression (Fig. 2E). In addition to *Chrdl1*, *Dand5* encoded another BMP antagonist whose expression was also increased in response to TGF-β in breast cancer cells with diminished ShcA expression (Fig. 2F). *Noggin* expression was found to be elevated in ShcA$^{low}$ cells in the absence of TGF-β treatment (Fig. 2F).

Currently, no data that link the inhibitory activity of Chrdl1 toward BMPs and breast cancer progression have been reported. These findings prompted us to investigate Chrdl1 as a modulator of malignant breast cancer phenotypes. To validate the gene expression data, we performed RT-qPCR analysis on total RNA isolated from NMuMG-ErbB2/rtTA/ShcA-KD cells treated with or without doxycycline and stimulated with TGF-β for 0, 3, or 24 h. These data revealed a significant induction of *Chrdl1* mRNA levels after 24 h of TGF-β treatment specifically when ShcA levels were reduced (Fig. 2G). Similarly, when conditioned medium harvested from the same experiment was subjected to ELISA analysis, secreted Chrdl1 levels were increased in this context (Fig. 2H).

Breast tumors possessing gene expression patterns indicative of active TGF-β signaling belong predominantly to the HER2$^+$ or basal-like subtypes (35). Moreover, breast cancer patients with tumors exhibiting an active TGF-β signature exhibited poor relapse-free and overall survival (35). To extend our analyses of Chrdl1 expression, an additional HER2$^+$ (NIC) model and two basal-like (MDA-MB-231 and BT549) breast cancer cell lines were chosen. We transiently reduced ShcA levels using siRNA-mediated approaches in NIC, MDA-MB-231, and BT549 cells and confirmed efficient knockdowns by immunoblot analysis (Fig. 3A to C). Subsequently, all cells were incubated in the absence or presence of TGF-β for 24 h, and conditioned medium was harvested and subjected to ELISAs to quantify secreted Chrdl1 levels. We observed uniform increases in secreted Chrdl1 following TGF-β stimulation in all breast cancer cell lines with low ShcA levels

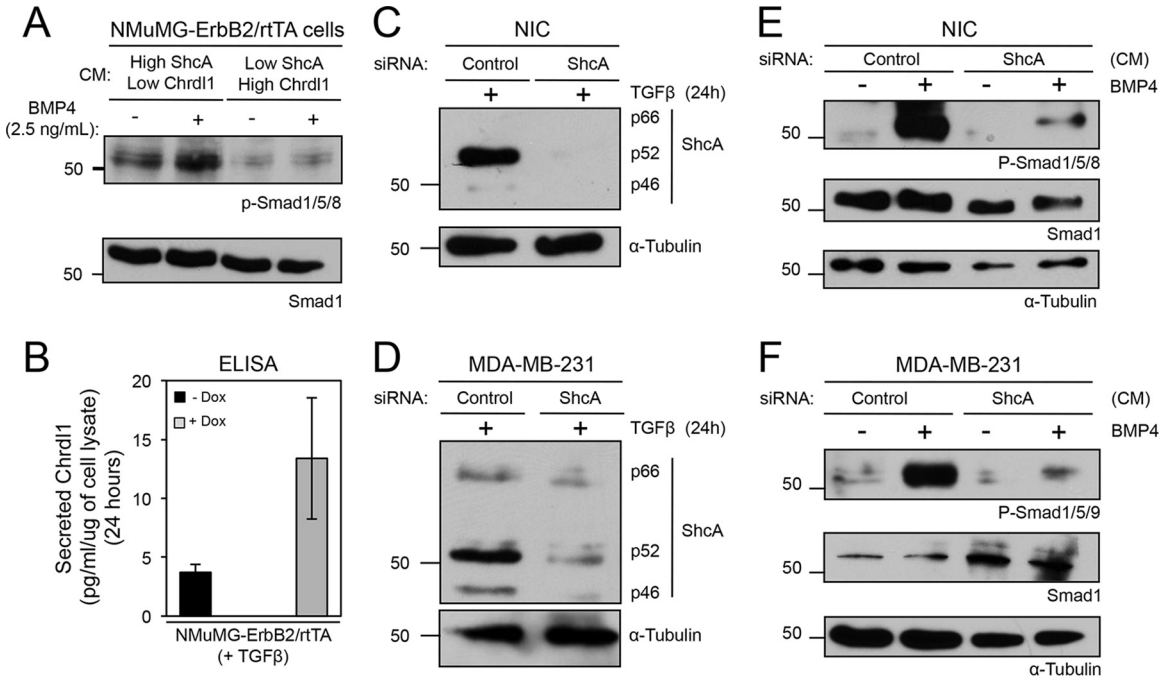


**FIG 5** Conditioned medium containing Chrdl1 suppresses BMP4-induced Smad phosphorylation in breast cancer cells. (A) Immunoblot analysis with antibodies specific for phospho-Smad and total Smad1 in cells with high or low Chrdl1 levels following BMP4 treatment (30 min, 2.5 ng/ml). (B) ELISAs were performed on conditioned media from the indicated cell populations. Secreted Chrdl1 concentrations were normalized to protein concentrations from whole-cell protein lysates. (C and D) Immunoblot analysis with antibodies against ShcA was performed on NIC (C) and MDA-MB-231 (D) breast cancer cells that were transfected with scrambled control or ShcA-specific siRNAs and stimulated with TGF-β (2 ng/ml) or not stimulated for 24 h. Conditioned medium was collected and added to serum-starved NIC and MDA-MB-231 cells, which were left untreated or immediately stimulated with BMP4 (2.5 ng/ml) for 30 min. (E and F) NIC (E) or MDA-MB-231 (F) breast cancer cells were lysed and subjected to immunoblot analysis with antibodies specific for phospho-Smad1/5/8 (NIC), phospho-Smad1/5/9 (MDA-MB-231), or total Smad1. In all cases, α-tubulin was used as a loading control.

(Fig. 3D to F). These results suggest that a combination of reduced ShcA levels and TGF-β treatment causes a uniform upregulation of Chrdl1 expression in multiple mouse and human breast cancer cells.

**Stable ShcA knockdown increases Chrdl1 protein expression *in vivo*.** Next, we determined if Chrdl1 protein expression was elevated *in vivo* using ErbB2-expressing breast cancer cells with stably diminished ShcA levels (9). NMuMG-ErbB2/ShcA$^{high}$ cells represent pooled populations infected with a retrovirus vector harboring shRNAs against the luciferase gene as a control, while NMuMG-ErbB2/ShcA$^{low}$ cells constitutively express ShcA gene-targeting shRNAs; therefore these cell populations are distinct from the doxycycline-inducible system described above. We performed IHC staining of ShcA and Chrdl1 on paraffin-embedded primary mammary tumors from mice injected with NMuMG-ErbB2/ShcA$^{high}$ or NMuMG-ErbB2/ShcA$^{low}$ breast cancer cells. Importantly, we have previously shown that NMuMG-ErbB2 mammary tumors are constantly under the influence of TGF-β (9). Strong Chrdl1 staining was uniformly distributed in tumor tissues harboring reduced ShcA levels (NMuMG-ErbB2/ShcA$^{low}$), whereas Chrdl1 levels were low in mammary tumors expressing endogenous levels of ShcA (NMuMG-ErbB2/ShcA$^{high}$) (Fig. 4). These results demonstrate that induction of Chrdl1 expression is associated with reduced levels of ShcA *in vivo*.

**Chrdl1 suppresses BMP4-induced Smad phosphorylation in breast cancer cells.** Chrdl1 is an inhibitor of BMP signaling with high affinity for BMP4 (21). For this reason, we chose to stimulate ErbB2/rtTA/ShcA-KD cells using recombinant BMP4 protein in the presence of conditioned medium containing low or high levels of Chrdl1. First, ErbB2/rtTA/ShcA-KD cells were plated in the presence or absence of doxycycline for 72 h and subsequently stimulated with TGF-β for 24 h. Conditioned media containing low or high levels of secreted Chrdl1 expression were collected and added to fresh cultures of ErbB2/rtTA/ShcA-KD cells that had been serum starved overnight. Finally, breast cancer cells were treated with BMP4 for 30 min, and both cell lysates and conditioned media were harvested to perform immunoblot and ELISA analyses. In breast cancer cells possessing high ShcA levels (ShcA$^{high}$ cells) and low Chrdl1 expression, increased levels of phospho-Smad1/5/8 were observed following BMP4 stimulation (Fig. 5A). Conversely, when cells were stimulated with BMP4 in the context of diminished ShcA levels (ShcA$^{low}$ cells) and high Chrdl1 expression, BMP4 treatment failed to induce the phosphorylation of Smad1/5/8 (Fig. 5A). Interestingly, the basal levels of phospho-Smad1/5/8 were reduced under conditions where secreted Chrdl1 levels were high (Fig. 5A). Elevated Chrdl1 levels in ErbB2-expressing breast cancer cells, with induced ShcA loss, were confirmed following TGF-β treatment by ELISA (Fig. 5B).

Similar experiments were performed using conditioned media harvested from NIC and MDA-MB-231 breast cancer cells. Transient knockdown of ShcA in each cell population was confirmed by immunoblot analysis (Fig. 5C and D). Responder NIC and MDA-MB-231 cells were incubated with conditioned medium containing low or high levels of Chrdl1 and subsequently treated with or without BMP4. Immunoblot analysis revealed that BMP4-

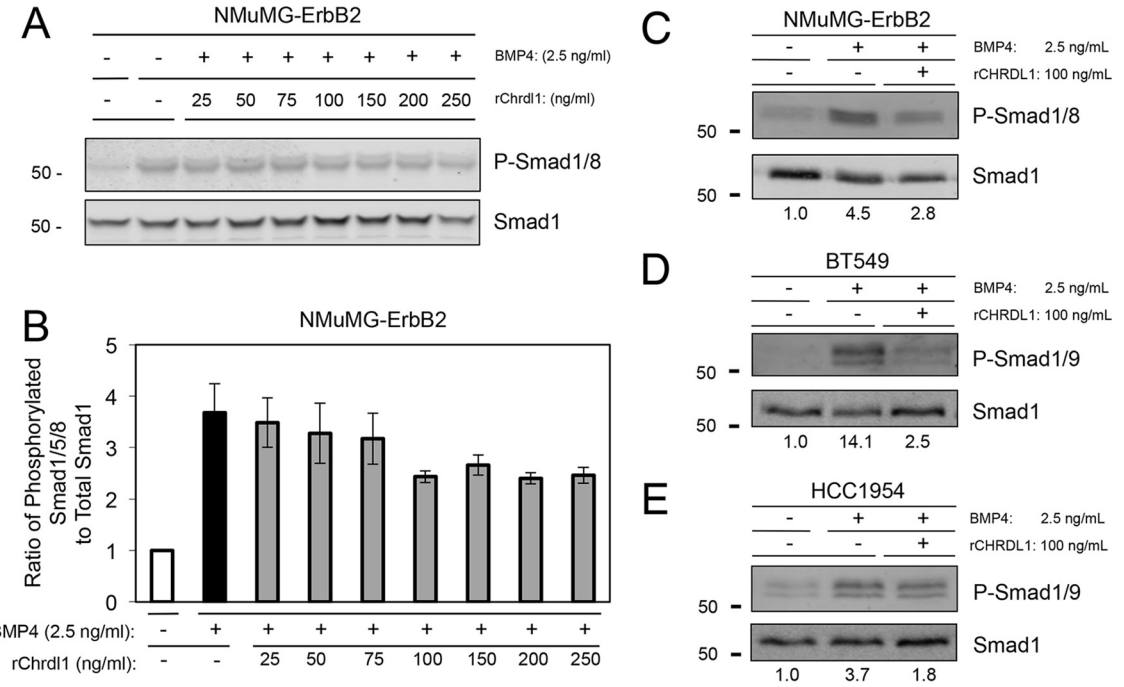


**FIG 6** Recombinant Chrdl1 diminishes BMP4-induced Smad phosphorylation in breast cancer cells. (A) Immunoblot analyses using antibodies against phospho-Smad1/8 and total Smad1 in NMuMG-ErbB2 breast cancer cells treated with BMP4 (30 min, 2.5 ng/ml) and increasing concentration of rChrdl1 (30 min, 25 to 250 ng/ml). (B) The ratio of phosphorylated Smad1/8 to total Smad1 protein in NMuMG-ErbB2 cells was measured using the Odyssey infrared imaging system, and the averaged fold increases relative to untreated controls (−BMP4 and −rChrdl1) from three independent experiments are shown. (C to E) Immunoblot analyses using antibodies against phospho-Smad and total Smad1 in NMuMG-ErbB2 (phospho-Smad1/8) (C), BT549 (phospho-Smad1/9) (D), and HCC1954 (phospho-Smad1/9) (E) breast cancer cells treated with BMP4 (30 min, 2.5 ng/ml) and rChrdl1 (30 min, 100 ng/ml). The ratio of phosphorylated Smads to total Smad1 protein in NMuMG-ErbB2 (C), BT549 (D), and HCC1954 (E) cells was measured using the Odyssey infrared imaging system and the fold increases relative to untreated controls (−BMP4 and −rChrdl1) are indicated at the bottom of each panel.

induced Smad1/5/8 (NIC) or Smad1/5/9 (MDA-MB-231) phosphorylation was significantly impaired when conditioned medium containing high Chrdl1 levels was used (Fig. 5E and F). These results indicate that Chrdl1-containing conditioned medium can suppress BMP4-mediated signaling in multiple breast cancer cell lines.

**Recombinant Chrdl1 attenuates BMP4-induced Smad phosphorylation in breast cancer cell lines.** The data accumulated thus far suggest that Chrdl1 secreted into the conditioned medium of breast cancer cells can blunt BMP4 signaling. However, it is conceivable that factors in the conditioned medium other than Chrdl1 are responsible for these effects. To directly implicate Chrdl1, we tested the ability of recombinant Chrdl1 (rChrdl1) to block BMP4-induced signaling in breast cancer cells. We first determined that 100 ng/ml of rChrdl1 was sufficient to maximally impair BMP4-stimulated phosphorylation of Smad1/8 in NMuMG-ErbB2 cells (Fig. 6A and B). Quantitative immunoblot analysis revealed that Smad1/8 (NMuMG-ErbB2) or Smad1/9 (BT549 and HCC1954) phosphorylation was uniformly induced by BMP4 treatment in all breast cancer cells and that the addition of rChrdl1 (100 ng/ml) blunted this response by approximately 50% in HCC1954 and NMuMG-ErbB2 cells and close to 100% in BT549 cells (Fig. 6C to E). We extended these analyses to BMP7-induced Smad phosphorylation and determined that 400 ng/ml of rChrdl1 was able to suppress Smad1/9 (MDA-MB-231 and HCC1954) or Smad1/8 (NMuMG-ErbB2) phosphorylation in response to BMP7 (50 ng/ml) treatment (Fig. 7A to F). These data confirm that Chrdl1 is sufficient to block BMP4- and BMP7-induced signaling in breast cancer cells.

**Chrdl1 dampens BMP4-induced migration in NMuMG-ErbB2 and BT549 cells.** Previous studies have shown that BMP4 enhances breast cancer cell migration (14). To determine if rChrdl1 could block this response, we performed time-lapse live-cell imaging of breast cancer cells (NMuMG-ErbB2 and BT549) cultured with BMP4 and in the presence or absence of rChrdl1. As a control, we used NMuMG-ErbB2 cells stimulated with TGF-β in the presence of Chrdl1. Low concentrations of Chrdl1 are insufficient to block TGF-β-induced signaling (21), and we have confirmed, using multiple breast cancer cell lines, that rChrdl1 (100 ng/ml) fails to blunt TGF-β-induced Smad2/3 phosphorylation (Fig. 7G to I).

As expected, NMuMG-ErbB2 or BT549 breast cancer cells stimulated with either BMP4 or TGF-β exhibited enhanced migration (Fig. 8). When these cells were cotreated with BMP4 and rChrdl1, migration was severely impaired by the BMP antagonist (Fig. 8A and C). In contrast, rChrdl1 was insufficient to impair TGF-β-induced migration of NMuMG-ErbB2 breast cancer cells (Fig. 8B). Thus, rChrdl1 efficiently impairs BMP4-induced migration in cell lines representative of different breast cancer subtypes.

**Chrdl1 suppresses BMP4-induced invasion in HER2$^+$ and basal-like breast cancer cells.** We next subjected HER2$^+$ (HCC1954) and basal-like (BT549) human breast cancer cell lines to cell invasion assays following BMP4 treatment, in the presence or absence of rChrdl1. In agreement with previous findings (15),

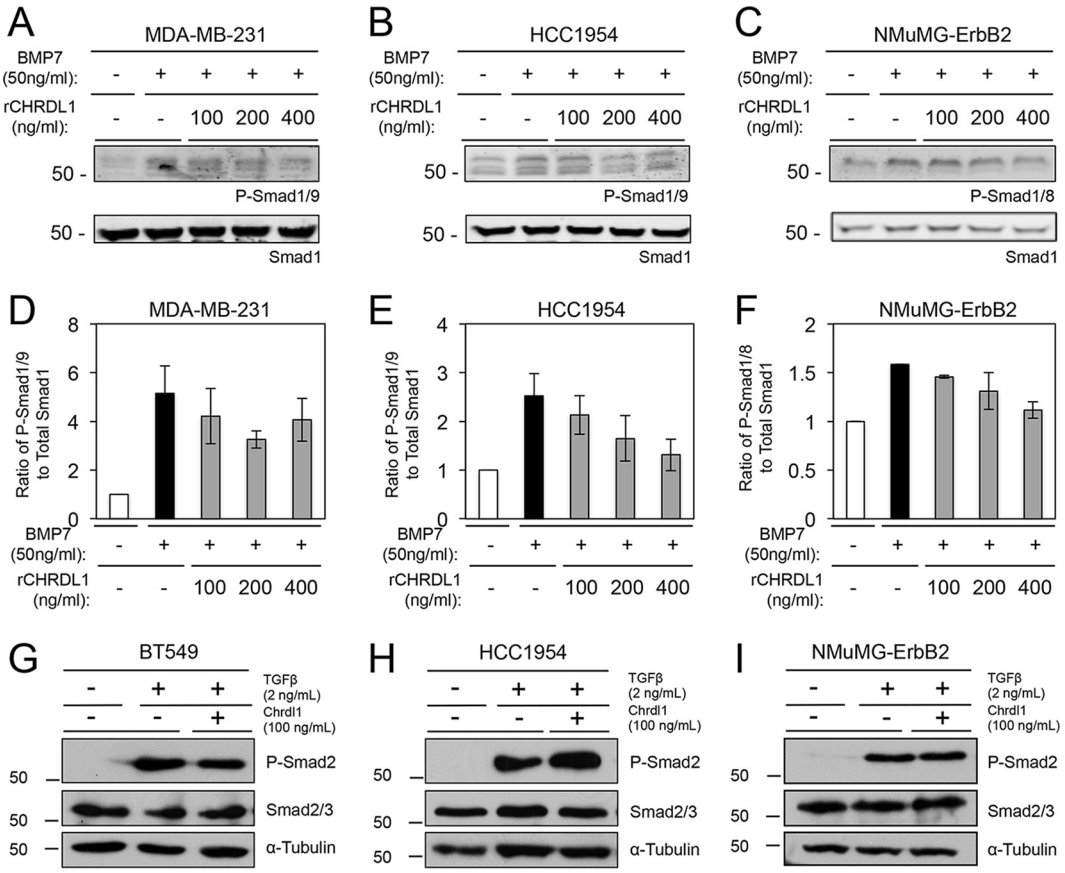


**FIG 7** Recombinant Chrdl1 suppresses BMP7-induced Smad1/8 phosphorylation in mouse breast cancer cells and Smad1/9 phosphorylation in human breast cancer cells but fails to block TGF-β-induced signaling. (A to C) Immunoblot analyses using antibodies against phospho-Smad and total Smad1 in MDA-MB-231 (phospho-Smad1/9) (A), HCC1954 (phospho-Smad1/9) (B), and NMuMG-ErbB2 (phospho-Smad1/8) (C) breast cancer cells treated with BMP7 (60 min, 50 ng/ml) and increasing concentrations of rChrdl1 (60 min, 100 to 400 ng/ml). (D to F) The ratio of phosphorylated Smads to total Smad1 protein in MDA-MB-231 (D), HCC1954 (E), and NMuMG-ErbB2 (F) breast cancer cells was measured using the Odyssey infrared imaging system, and the averaged fold increases relative to untreated controls (−BMP7 and −rChrdl1) from three independent experiments are shown. (G to I) BT549 (G), HCC1954 (H), and NMuMG-ErbB2 (I) breast cancer cells were serum starved overnight and stimulated with TGF-β (2 ng/ml) (+) or not stimulated (−) in the presence (+) or absence (−) of recombinant Chrdl1 (100 ng/ml) for 30 min. Immunoblot analyses were performed with antibodies against phospho-Smad2 and total Smad2/3. In all cases, α-tubulin was used as a loading control.

both HCC1954 and BT549 breast cancer cells displayed enhanced invasion in response to BMP4 compared to unstimulated cells (Fig. 9A) (15). BMP4 stimulation resulted in a 2.0-fold increase in HCC1954 invasion and a 2.0- to 2.5-fold increase in BT549 cell invasion compared to that in unstimulated cultures (Fig. 9A). BMP4-induced invasion of both HCC1954 and BT549 cells was significantly inhibited by the addition of rChrdl1 relative to that in cells treated with BMP4 alone (Fig. 9A). Together, these results demonstrate that BMP4 enhances the invasion of both HCC1954 and BT549 breast cancer cells, and this response can be abolished by rChrdl1.

**BMP4-induced gelatin matrix degradation is impaired by Chrdl1.** Cancer cell invasion is associated with the formation of specialized degradative structures, called invadopodia, that digest extracellular matrix (ECM) (36, 37) via a metalloproteinase-dependent mechanism (38, 39). Previous studies have demonstrated that invadopodium-mediated extracellular matrix degradation is directly correlated with the invasive potential of breast cancer cells (40–42). Based on these observations, we hypothesized that cells stimulated with BMP4 would exhibit a greater extent of ECM degradation than unstimulated cells. To test this, BMP4-pretreated NMuMG-ErbB2 and BT549 breast cancer cells were plated on fluorescent-gelatin-matrix-coated coverslips for 24 h. Coverslips were imaged using immunofluorescence microscopy, and the area of gelatin matrix degradation was quantified (Fig. 9B). BMP4-stimulated breast cancer cells produce multiple regions of degradation compared to unstimulated cells, where almost no matrix degradation was observed. Thus, the total area of gelatin degradation is significantly higher in BMP4-treated breast cancer cells than in unstimulated cells. Moreover, this BMP4-induced effect was almost completely abolished when cells were treated with Chrdl1 (Fig. 9B).

**Chrdl1 diminishes BMP4-induced MMP2 and MMP9 activity.** ECM degradation by invadopodia is dependent on MMP14 (39), a transmembrane metalloproteinase that can activate the soluble metalloproteinases MMP2 and MMP9, which can degrade gelatin (43, 44). To determine if BMP4 induces expression of these metalloproteinases, we performed RT-qPCR analyses in BMP4-stimulated breast cancer cells. Our results indicate that BMP4 treatment (24 and 48 h) does not induce *MMP2*, *MMP9*, or

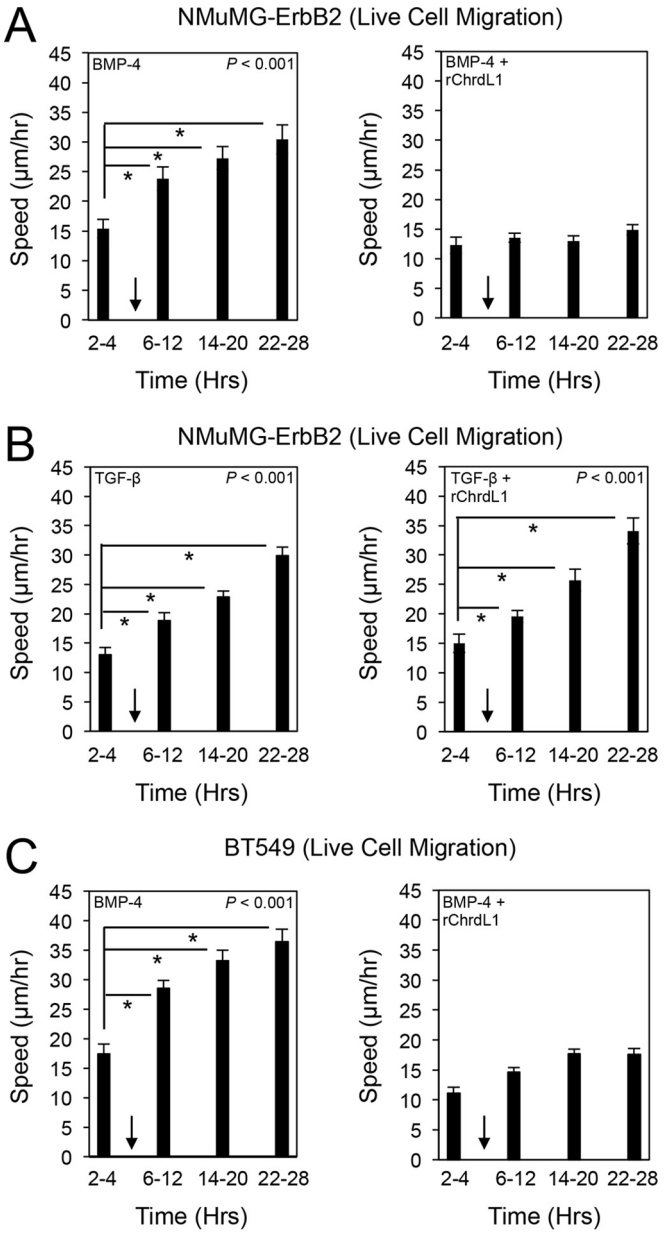


**FIG 8** Chrdl1 blocks BMP4-induced but not TGF-β-induced cell migration of NMuMG-ErbB2 cells and BT549 breast cancer cells. Analysis of cellular velocity as measured by manual tracking of NMuMG-ErbB2 and BT549 cells is shown. Cells were stimulated with BMP4 (2.5 ng/ml) (A and C) or TGF-β (2 ng/ml) (B) in the absence (left panels) or presence (right panels) of rChrdl1 (100 ng/ml). The graphs represent the mean cellular velocity from one representative experiment (four experiments for NMuMG-ErbB2 cells and three experiments for BT549 cells). The arrow in each panel indicates the time that ligand (BMP4 or TGF-β), in the presence or absence of rChrdl1, was added to the cultures. *, $P < 0.001$.

*MMP14* mRNA expression (Fig. 10A). To explore the possibility that BMP4 induces MMP activity, conditioned media from NMuMG-ErbB2 and BT549 breast cancer cells that were treated with BMP4 for 48 h were subjected to zymography assays. In contrast to the case for *MMP2* and *MMP9* expression, 48 h of BMP4 treatment resulted in a clear induction of MMP2 and MMP9 enzymatic activity in both cell lines, which was effectively blocked by Chrdl1 (Fig. 10B and C).

**High levels of *Chrdl1* expression are associated with better outcome in breast and lung cancer patients.** To determine the clinical relevance of our observations, we investigated whether *Chrdl1* expression was prognostic of outcome in patients with diverse cancers using publically available gene expression data sets (29–31). In breast cancer, *Chrdl1* mRNA expression was found to be higher in basal and luminal A breast cancers than in HER2$^+$ or luminal B disease (Fig. 11A). We used the Kaplan-Meier method and log rank test to analyze correlations between *Chrdl1* mRNA levels and the overall survival (Fig. 11B), disease-free survival (Fig. 11C), or distant metastasis-free survival (Fig. 11D) of breast cancer patients ($n$ = 1,115). Patients were split into high- and low-*Chrdl1* mRNA-expressing groups based upon median *Chrdl1* mRNA expression across all samples. Our findings revealed that breast cancer patients with high-*Chrdl1* mRNA-expressing tumors had significantly greater overall, disease-free, and distant metastasis-free survival times than patients with low-*Chrdl1* mRNA-expressing tumors (Fig. 11B to D). The relationship between *Chrdl1* expression and overall survival in 1,926 lung cancer patients, 1,581 ovarian cancer patients, and 1,305 gastric cancer patients was also examined (Fig. 12). Similar to the results for breast cancer, lung cancer patients with high-*Chrdl1* mRNA-expressing tumors had significantly greater overall survival times than those with low-*Chrdl1* mRNA-expressing tumors (Fig. 12A). In contrast, *Chrdl1* mRNA levels were not prognostic of better overall survival in ovarian and gastric cancer patients (Fig. 12B and C). Thus, the ability of Chrdl1 to impair malignant cancer phenotypes may be cancer and context specific.

## DISCUSSION

We previously demonstrated that TGF-β- and ErbB2-mediated breast cancer cell migration and invasion relied on the ShcA adaptor protein (8, 9). To understand how ShcA signaling contributes to TGF-β-induced gene expression changes in ErbB2-expressing breast cancer cells, we developed a system to stably knock down ShcA expression in a doxycycline-inducible manner. The *Chrdl1* gene emerged as a gene that is upregulated in numerous breast cancer cells (HER2$^+$ and basal subtype) following TGF-β stimulation, but only in the context of reduced ShcA signaling. Moreover, in ErbB2-expressing mammary tumors that are under the influence of constitutive TGF-β derived from the microenvironment, Chrdl1 levels were dramatically increased in the absence of ShcA *in vivo*. We show that BMP4 increases the migratory, invasive, and matrix-degradative phenotypes of breast cancer cells, which are effectively blocked by Chrdl1. In keeping with this biological activity, high Chrdl1 expression in breast cancer is associated with better outcomes for patients with this disease.

Chrdl1 functions as a BMP inhibitor, exhibiting the highest affinity for BMP4 and requiring much higher concentrations to impair other BMP and TGF-β family members (21). Our data confirmed that both conditioned medium from breast cancer cells containing high Chrdl1 levels and rChrdl1 suppress BMP4-induced Smad1/5/8 phosphorylation. Moreover, at the concentrations of rChrdl1 utilized in these studies, we failed to see suppression of TGF-β-induced Smad2/3 phosphorylation. BMPs can influence numerous aspects of tumor growth and metastasis, and levels of specific family members, such as BMP4 and BMP7, are frequently elevated in breast cancers (10, 14, 45). Indeed, it has been shown that BMP4 positively regulates angiogenesis via enhanced endothelial cell migration and tube formation *in vitro* (46,

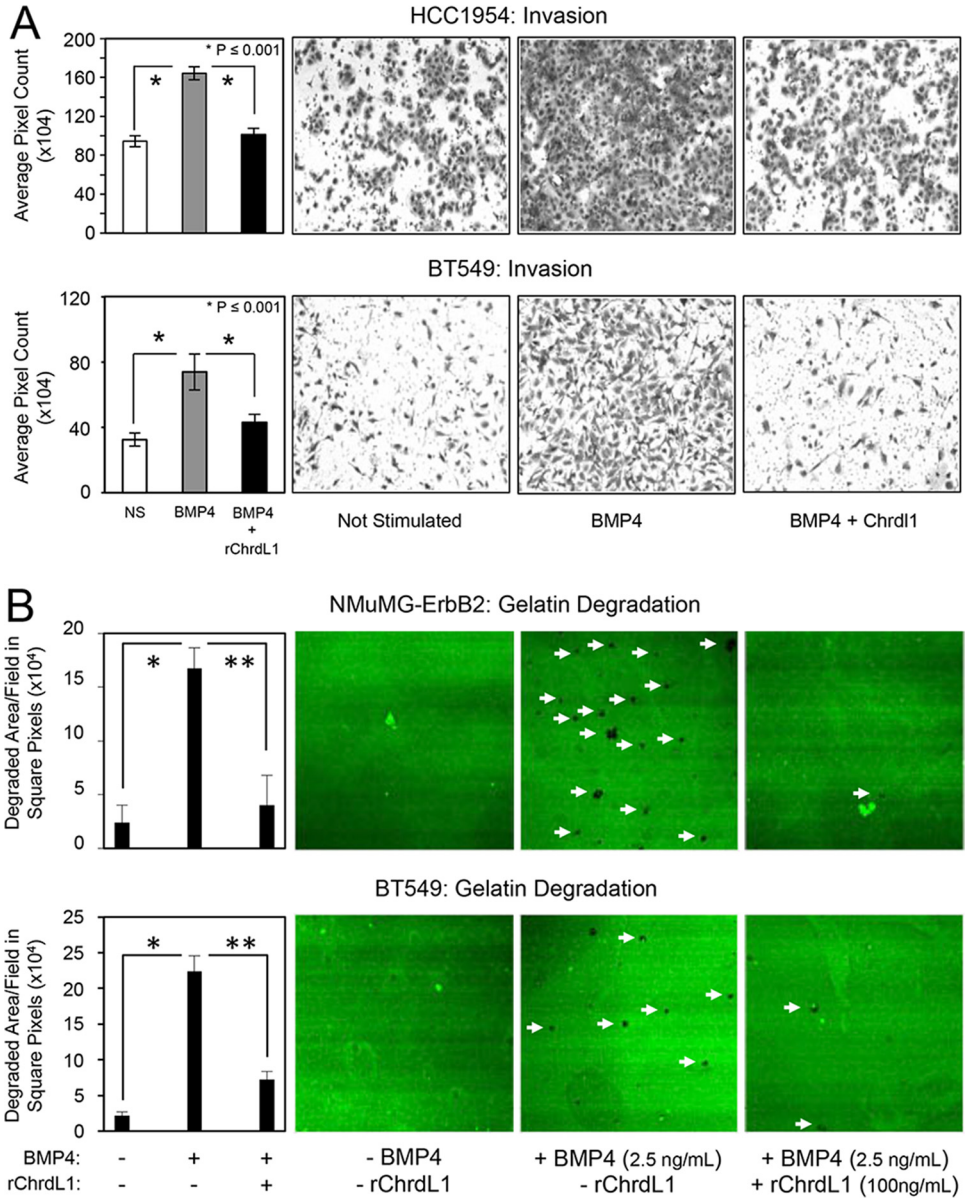


**FIG 9** Chrdl1 impairs BMP4-induced breast cancer invasion and gelatin degradation. (A) Boyden chamber invasion assays were performed with HCC1954 and BT549 cells. The data represent the average from three (HCC1954) or four (BT549) independent experiments performed in triplicate. Representative images from each breast cancer cell line, under each condition, are shown. *, $P < 0.001$. (B) NMuMG-ErbB2 and BT549 cells treated with or without BMP4, in the presence or absence of Chrdl1, for 24 h were cultured on glass coverslips coated with green fluorescent protein (GFP) fluorescent-gelatin matrix. Cells were fixed and images captured using confocal microscopy. Quantification of matrix degradation is illustrated in the graph, and representative images from each experimental condition are shown. The data represent two independent experiments (20 images were quantified for each condition in each independent experiment). Arrows indicate areas of gelatin degradation. NMuMG-ErbB2: *, $P = 0.0164$; **, $P = 0.044$. BT549: *, $P = 0.0373$; ** $P = 0.027$.

47). Thus, it is conceivable that loss of BMP4-mediated signaling, via induction of Chrdl1 expression, may account for the reduced endothelial recruitment observed in mammary tumors harboring diminished ShcA expression (9).

BMPs can promote the migration and invasion of breast cancer cells *in vitro* (13–15, 48–50). By performing time-lapse live-cell imaging, we demonstrated that treatment with either BMP4 or TGF-β promoted the migration of NMuMG-ErbB2 and BT549 breast cancer cells. We further showed, using $HER2^+$ and basal breast cancer cells, that Chrdl1 suppressed BMP4-induced migration but failed to diminish TGF-β-mediated migration. These data are consistent with results showing that distinct BMP inhibitors, such as Chordin or Noggin, can inhibit BMP-induced migration in melanoma and ovarian cancer cell lines (47, 51, 52).

Our data also reveal that BMP4 treatment of BT549 and HCC1954 cells can induce a significant increase in cell invasion, as was previously shown for HCC1954 cells (15). In agreement with previous studies showing that inhibition of BMP4 signaling diminishes the invasion of malignant melanoma cells (47), we demonstrated that Chrdl1 significantly reduced BMP4-induced breast cancer cell invasion. Recent evidence implicates Smad-independent pathways as regulators of BMP4-induced migration and in-

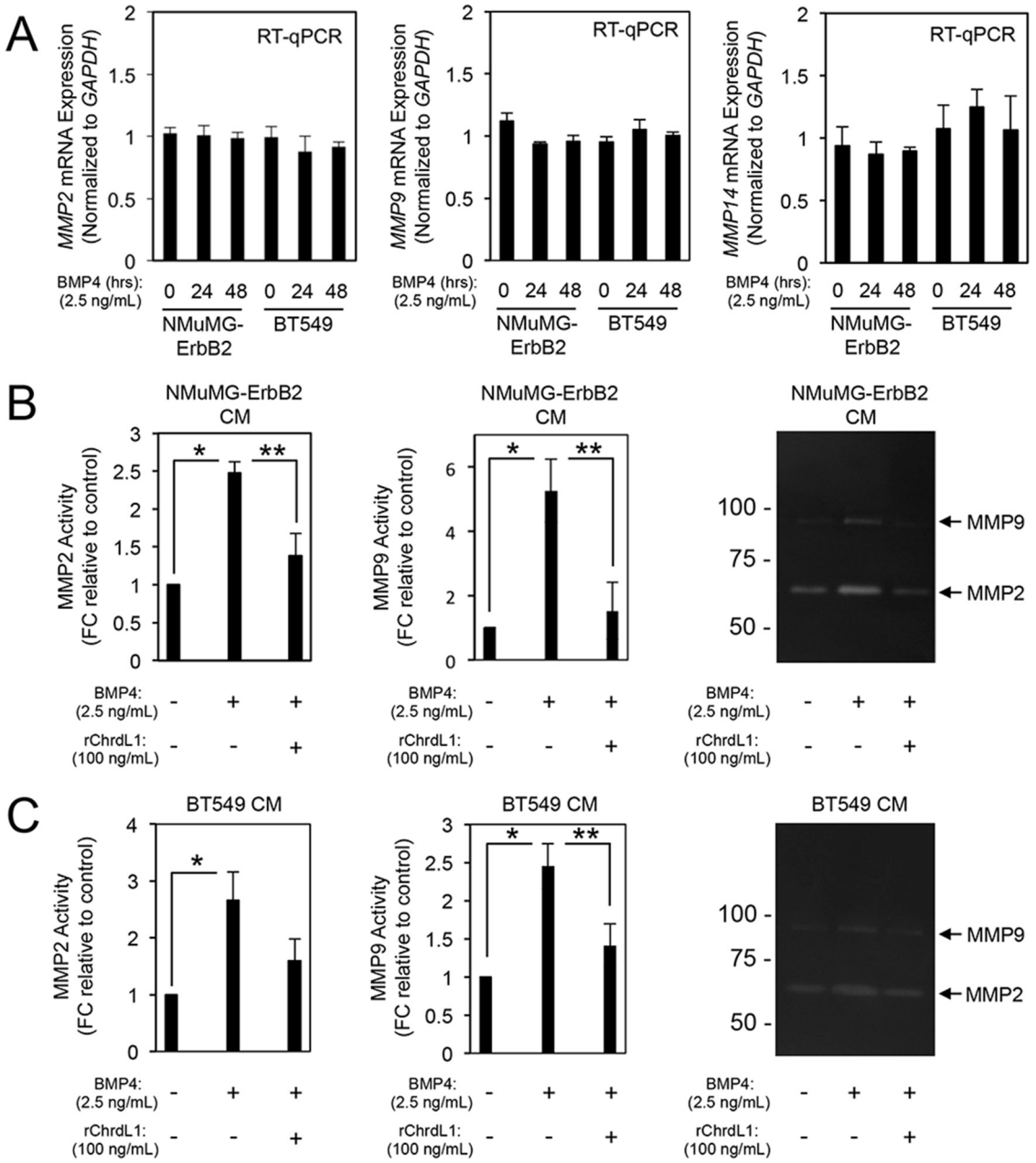


**FIG 10** Chrdl1 impairs BMP4-induced MMP2 and MMP9 enzymatic activity. (A) NMuMG-ErbB2 and BT549 breast cancer cells were stimulated with BMP4 (2.5 ng/ml) or not stimulated for 24 and 48 h. MMP2, MMP9, and MMP14 mRNA levels were measured by RT-qPCR. The data represent the means from three independent experiments performed in triplicate. No statistically significant differences in MMP mRNA expression were observed following BMP4 stimulation. (B and C) Conditioned media (CM) from NMuMG-ErbB2 (B) and BT549 (C) breast cancer cells stimulated with BMP4 (2.5 ng/ml) or not stimulated, in the presence or absence of rChrdl1 (100 ng/ml), for 48 h were harvested and analyzed for MMP activity by gelatin zymography. The gels were photographed, and band intensities were digitally quantified. The data represent the mean band intensity for each condition from three (B) or four (C) independent experiments. (B, left) *, $P < 0.0022$; **, $P < 0.024$; (B, middle) *, $P < 0.022$; **, $P < 0.029$; (C, left) *, $P < 0.045$; (C, middle) *, $P < 0.016$; **, $P < 0.045$.

vasion. CCN6, a secreted matricellular protein, has been shown to associate with and antagonize the promigratory and proinvasive functions of BMP4 in MDA-MB-231 breast cancer cells via inhibition of TAK1 and p38 MAPK signaling (16). Another putative mechanism for BMP4-induced cancer cell invasion involves downstream activation of MMP expression, including expression of MMP1, MMP3, and MMP14 (13, 14). More recently, it was shown that BMP also indirectly influences breast cancer invasion. Indeed, BMP4-stimulated cancer-associated fibroblasts (CAFs) secrete proinflammatory cytokines and MMPs that induce the invasive properties of breast cancer cells (53).

Using a gelatin matrix degradation assay, we further demonstrated that BMP4 promotes cellular invasion, an effect that is blunted by Chrdl1. In breast cancer cells, actin-rich membrane protrusions, called invadopodia, have been characterized as important structures required for cancer cell invasion through ma-

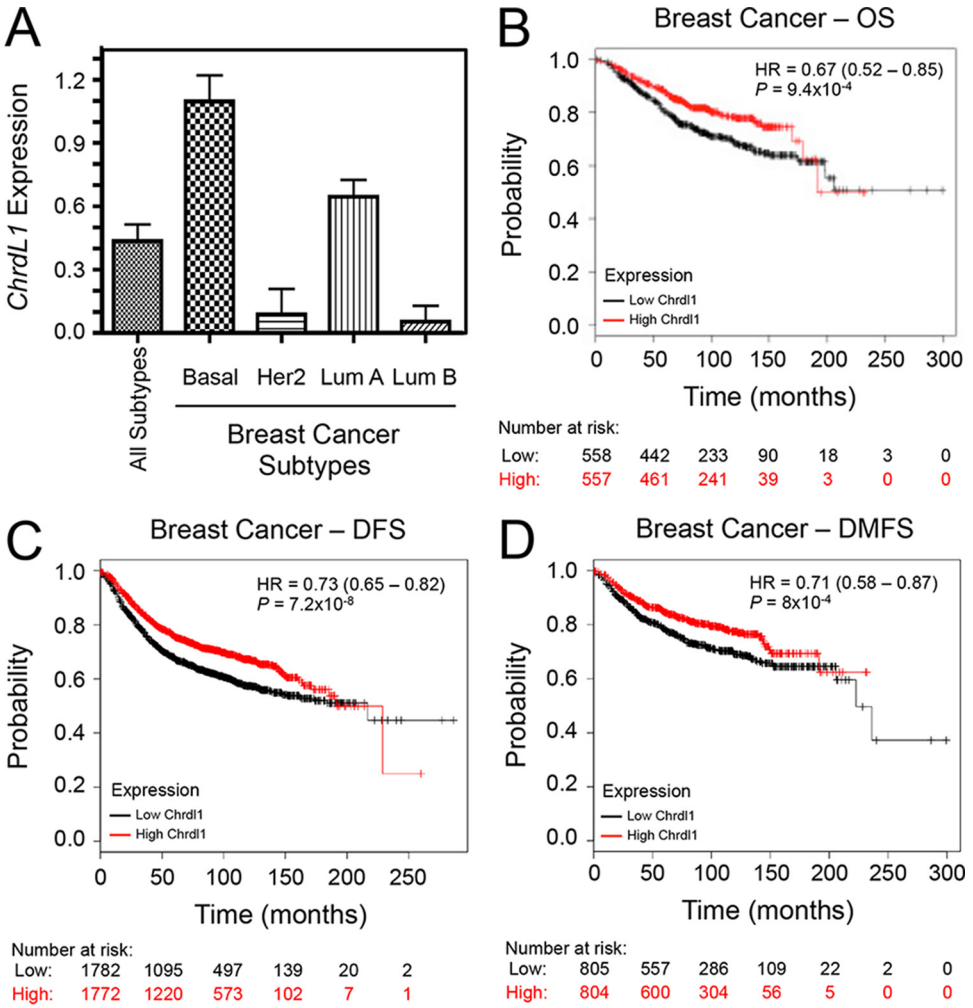


**FIG 11** Correlations between *Chrdl1* expression and clinical outcomes in breast cancer patients. (A) *Chrdl1* mRNA expression is elevated in the basal and luminal A subtypes. The average *Chrdl1* mRNA levels in all breast cancer subtypes was compared to the average *Chrdl1* mRNA levels in each individual subtype (Lum A, luminal A; Lum B, luminal B). (B to D) Kaplan-Meier survival curves comparing *Chrdl1* expression with overall survival (OS) (B), disease-free survival (DFS) (C), or distant metastasis-free survival (DMFS) (D) in breast cancer ($n = 1{,}115$ patients). *P* values were calculated using the log rank test between patients with high versus low *Chrdl1* expression by using a median split.

trix (36, 37). Maturation of invadopodia requires cell membrane localization of MMP14 (MT1-MMP), a metalloproteinase known to activate MMP2 and MMP9 (39, 44). However, very little is known about how BMPs influence the formation of degradative structures such as invadopodia. Our results revealed that BMP4 induces MMP2 and MMP9 enzymatic activity in breast cancer cells and increases their ability to degrade a gelatin matrix. These responses were effectively blocked by addition of rChrdl1. Mechanisms underlying MMP-dependent matrix degradation are now emerging. Recently, a link between CDCP1 expression and the localization of MMP14 (MT1-MMP) to invadopodia structures has been established (54). That study reports that knockdown of CDCP1 reduces the accumulation of MMP14 (MT1-MMP) at invadopodia without affecting its expression, which as a result decreases gelatin matrix degradation. Interestingly, there is evidence that BMP4 induces CDCP1 expression through extracellular signal-regulated kinase (ERK) pathway activation (55). Therefore, it is conceivable that BMP4 enhances matrix degradation through induction of CDCP1 expression and subsequent MMP14 (MT1-MMP) localization to invadopodia. However, further investigation will be needed to elucidate the exact mechanism by which BMP4 induces breast cancer cell invasion. Thus, our data highlight a new tumor-intrinsic mechanism through which BMPs stimulate breast cancer invasion. Our data are consistent with a recent publication demonstrating that a BMP antagonist, DMH1, is capable of suppressing mammary tumor cell proliferation, increasing apoptosis, and impairing lung metastasis (56).

It is important to note that not all BMP antagonists are thought to suppress breast cancer metastasis. For example, the BMP ligand antagonist Coco enhances the self-renewal capability of metastasis-initiating breast cancer cells within the lung, and knockdown of Coco in MDA-MB-231 cells was sufficient to block lung metastasis (57). Overexpression of another BMP inhibitor, Noggin, can enhance the ability of breast cancer cells to form bone metastases (58). In addition, BMP4 has recently been attributed tumor-suppressive functions via its ability to block the activity of infiltrating myeloid-derived suppressor cells (MDSCs) (59). Thus, BMP4 signaling and its regulation by

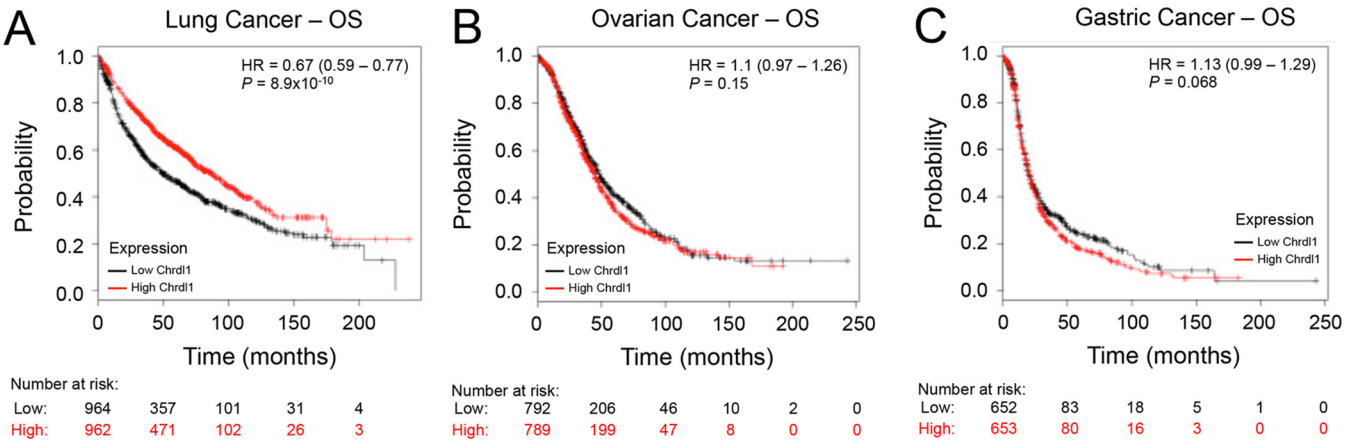


**FIG 12** Clinical correlations between *Chrdl1* expression and overall survival of lung, ovarian, and gastric cancer patients. Kaplan-Meier survival curves comparing *Chrdl1* expression with overall survival in lung cancer ($n = 1{,}926$) (A), ovarian cancer ($n = 1{,}581$) (B) and gastric cancer ($n = 1{,}305$) (C) patients are shown. *P* values were calculated using the log rank test between patients with high versus low *Chrdl1* expression by using a median split.

BMP antagonists can have complex and context-dependent effects on breast cancer progression.

In this regard, our analysis of clinical data sets provides the first evidence that Chrdl1 may serve as a useful prognostic indicator of good outcome in specific types of cancer. Kaplan-Meier analysis revealed that breast cancer patients whose tumors expressed high *Chrdl1* levels had significantly longer overall, disease-free, and distant metastasis-free survival times than patients whose tumors expressed low levels of *Chrdl1*. Interrogation of a lung cancer data set revealed a similar correlation between high *Chrdl1* levels and longer overall survival times. Interestingly, similar to studies cited above for breast cancer, several reports provide evidence that BMP signaling promotes the growth and progression of lung cancer (60). In this regard, although BMP4 has not been extensively studied in lung cancer, BMP2 has repeatedly been positively associated with lung cancer progression (61, 62). Conversely, we did not observe a positive correlation between *Chrdl1* and better overall survival in ovarian and gastric cancer patients. In fact, high levels of *Chrdl1* trended with poorer overall survival in these cancers; however, the differences in the survival curves were small and did not reach significance. These clinical associations are consistent with a study showing that high BMP4 levels in ovarian cancer patients prior to chemotherapy was a prognostic factor for longer progression-free and overall survival times (63). At present, very little is known regarding BMP4 signaling activity and clinical outcomes in gastric cancer. Taken together, our data reveal the intriguing possibility that Chrdl1 levels are prognostic of good outcome in certain types of cancer, including breast cancer. These data are in agreement with the ability of Chrdl1 to impair BMP4-induced breast cancer cell migration and invasion.

It is interesting that breast tumors exhibiting gene expression profiles associated with active TGF-β signaling (constitutively active TβRI signature) belong mostly to the $HER2^+$ or basal-like subtypes and that these patients exhibit poor relapse-free and overall survival (35). The emergence of inhibitors that target receptor tyrosine kinases (RTKs) in $HER2^+$ and basal breast cancers would create a situation of diminished signaling downstream of RTKs akin to the situation we have achieved through reduction of ShcA expression. Given the prominent activation of TGF-β signaling in these subtypes, it would be interesting to examine Chrdl1 levels in breast tumors of patients receiving anti-RTK inhibitors (anti-ErbB2/EGFR inhibitors or anti-Met inhibitors).

## ACKNOWLEDGMENTS

We thank members of the Siegel laboratory for their valuable comments and suggestions. We are grateful to Charles Thevaranjan Vincent Rajadurai for his assistance with establishing the fluorescent gelatin degradation assay. We acknowledge support from the Goodman Cancer Research Centre Histology Core Facility for routine histology services. We thank Claire Brown and the McGill Life Science Complex Advanced BioImaging Facility for assistance with the time-lapse live-cell imaging analysis.

C.C.-D. acknowledges previous and current salary support from the McGill University Faculty of Medicine and the Défi Corporatif Canderel. P.M.S. recognizes previous salary support from the FRQS and is currently a William Dawson Scholar of McGill University.

## FUNDING INFORMATION

This research was supported by grants from the Association for International Cancer Research (AICR) (11-0204) and the Canadian Cancer Society Research Institute (CCSRI) (2011-700790) to P.M.S.

## REFERENCES

1. **Dawson SJ, Rueda OM, Aparicio S, Caldas C.** 2013. A new genome-driven integrated classification of breast cancer and its implications. EMBO J **32:**617–628. http://dx.doi.org/10.1038/emboj.2013.19.
2. **Prat A, Perou CM.** 2011. Deconstructing the molecular portraits of breast cancer. Mol Oncol **5:**5–23. http://dx.doi.org/10.1016/j.molonc.2010.11.003.
3. **Arteaga CL, Sliwkowski MX, Osborne CK, Perez EA, Puglisi F, Gianni L.** 2012. Treatment of HER2-positive breast cancer: current status and future perspectives. Nat Rev Clin Oncol **9:**16–32. http://dx.doi.org/10.1038/nrclinonc.2011.177.
4. **Muraoka RS, Koh Y, Roebuck LR, Sanders ME, Brantley-Sieders D, Gorska AE, Moses HL, Arteaga CL.** 2003. Increased malignancy of Neu-induced mammary tumors overexpressing active transforming growth factor β1. Mol Cell Biol **23:**8691–8703. http://dx.doi.org/10.1128/MCB.23.23.8691-8703.2003.
5. **Seton-Rogers SE, Lu Y, Hines LM, Koundinya M, LaBaer J, Muthuswamy SK, Brugge JS.** 2004. Cooperation of the ErbB2 receptor and transforming growth factor beta in induction of migration and invasion in mammary epithelial cells. Proc Natl Acad Sci U S A **101:**1257–1262. http://dx.doi.org/10.1073/pnas.0308090100.
6. **Siegel PM, Shu W, Cardiff RD, Muller WJ, Massague J.** 2003. Transforming growth factor β signaling impairs Neu-induced mammary tu-

morigenesis while promoting pulmonary metastasis. Proc Natl Acad Sci U S A **100:**8430–8435. http://dx.doi.org/10.1073/pnas.0932636100.
7. **Ueda Y, Wang S, Dumont N, Yi JY, Koh Y, Arteaga CL.** 2004. Overexpression of HER2 (erbB2) in human breast epithelial cells unmasks transforming growth factor beta-induced cell motility. J Biol Chem **279:** 24505–24513. http://dx.doi.org/10.1074/jbc.M400081200.
8. **Northey JJ, Chmielecki J, Ngan E, Russo C, Annis MG, Muller WJ, Siegel PM.** 2008. Signaling through ShcA is required for TGF-β and Neu/ErbB-2 induced breast cancer cell motility and invasion. Mol Cell Biol **28:**3162–3176. http://dx.doi.org/10.1128/MCB.01734-07.
9. **Northey JJ, Dong Z, Ngan E, Kaplan A, Hardy WR, Pawson T, Siegel PM.** 2013. Distinct phosphotyrosine-dependent functions of the ShcA adaptor protein are required for transforming growth factor beta (TGF-beta)-induced breast cancer cell migration, invasion, and metastasis. J Biol Chem **288:**5210–5222. http://dx.doi.org/10.1074/jbc.M112.424804.
10. **Alarmo EL, Kuukasjarvi T, Karhu R, Kallioniemi A.** 2007. A comprehensive expression survey of bone morphogenetic proteins in breast cancer highlights the importance of BMP4 and BMP7. Breast Cancer Res Treat **103:**239–246. http://dx.doi.org/10.1007/s10549-006-9362-1.
11. **Alarmo EL, Kallioniemi A.** 2010. Bone morphogenetic proteins in breast cancer: dual role in tumourigenesis? Endocr Relat Cancer **17:**R123–R139. http://dx.doi.org/10.1677/ERC-09-0273.
12. **Ehata S, Yokoyama Y, Takahashi K, Miyazono K.** 2013. Bi-directional roles of bone morphogenetic proteins in cancer: another molecular Jekyll and Hyde? Pathol Int **63:**287–296. http://dx.doi.org/10.1111/pin.12067.
13. **Ampuja M, Jokimaki R, Juuti-Uusitalo K, Rodriguez-Martinez A, Alarmo EL, Kallioniemi A.** 2013. BMP4 inhibits the proliferation of breast cancer cells and induces an MMP-dependent migratory phenotype in MDA-MB-231 cells in 3D environment. BMC Cancer **13:**429. http://dx.doi.org/10.1186/1471-2407-13-429.
14. **Guo D, Huang J, Gong J.** 2012. Bone morphogenetic protein 4 (BMP4) is required for migration and invasion of breast cancer. Mol Cell Biochem **363:**179–190. http://dx.doi.org/10.1007/s11010-011-1170-1.
15. **Ketolainen JM, Alarmo EL, Tuominen VJ, Kallioniemi A.** 2010. Parallel inhibition of cell growth and induction of cell migration and invasion in breast cancer cells by bone morphogenetic protein 4. Breast Cancer Res Treat **124:**377–386. http://dx.doi.org/10.1007/s10549-010-0808-0.
16. **Pal A, Huang W, Li X, Toy KA, Nikolovska-Coleska Z, Kleer CG.** 2012. CCN6 modulates BMP signaling via the Smad-independent TAK1/p38 pathway, acting to suppress metastasis of breast cancer. Cancer Res **72:** 4818–4828. http://dx.doi.org/10.1158/0008-5472.CAN-12-0154.
17. **Alarmo EL, Parssinen J, Ketolainen JM, Savinainen K, Karhu R, Kallioniemi A.** 2009. BMP7 influences proliferation, migration, and invasion of breast cancer cells. Cancer Lett **275:**35–43. http://dx.doi.org/10.1016/j.canlet.2008.09.028.
18. **Sakai H, Furihata M, Matsuda C, Takahashi M, Miyazaki H, Konakahara T, Imamura T, Okada T.** 2012. Augmented autocrine bone morphogenic protein (BMP) 7 signaling increases the metastatic potential of mouse breast cancer cells. Clin Exp Metastasis **29:**327–338. http://dx.doi.org/10.1007/s10585-012-9453-9.
19. **Brazil DP, Church RH, Surae S, Godson C, Martin F.** 2015. BMP signalling: agony and antagony in the family. Trends Cell Biol **25:**249–264. http://dx.doi.org/10.1016/j.tcb.2014.12.004.
20. **Walsh DW, Godson C, Brazil DP, Martin F.** 2010. Extracellular BMP-antagonist regulation in development and disease: tied up in knots. Trends Cell Biol **20:**244–256. http://dx.doi.org/10.1016/j.tcb.2010.01.008.
21. **Nakayama N, Han CE, Scully S, Nishinakamura R, He C, Zeni L, Yamane H, Chang D, Yu D, Yokota T, Wen D.** 2001. A novel chordin-like protein inhibitor for bone morphogenetic proteins expressed preferentially in mesenchymal cell lineages. Dev Biol **232:**372–387. http://dx.doi.org/10.1006/dbio.2001.0200.
22. **Dupuy F, Griss T, Blagih J, Bridon G, Avizonis D, Ling C, Dong Z, Siwak DR, Annis MG, Mills GB, Muller WJ, Siegel PM, Jones RG.** 2013. LKB1 is a central regulator of tumor initiation and pro-growth metabolism in ErbB2-mediated breast cancer. Cancer Metab **1:**18. http://dx.doi.org/10.1186/2049-3002-1-18.
23. **Ngan E, Northey JJ, Brown CM, Ursini-Siegel J, Siegel PM.** 2013. A complex containing LPP and alpha-actinin mediates TGFbeta-induced migration and invasion of ErbB2-expressing breast cancer cells. J Cell Sci **126:**1981–1991. http://dx.doi.org/10.1242/jcs.118315.
24. **Rose AA, Annis MG, Dong Z, Pepin F, Hallett M, Park M, Siegel PM.** 2010. ADAM10 releases a soluble form of the GPNMB/Osteoactivin extracellular domain with angiogenic properties. PLoS One **5:**e12093. http://dx.doi.org/10.1371/journal.pone.0012093.
25. **Tabariès S, Dupuy F, Dong Z, Monast A, Annis MG, Spicer J, Ferri LE, Omeroglu A, Basik M, Amir E, Clemons M, Siegel PM.** 2012. Claudin-2 promotes breast cancer liver metastasis by facilitating tumor cell interactions with hepatocytes. Mol Cell Biol **32:**2979–2991. http://dx.doi.org/10.1128/MCB.00299-12.
26. **Rose AA, Pepin F, Russo C, Abou Khalil JE, Hallett M, Siegel PM.** 2007. Osteoactivin promotes breast cancer metastasis to bone. Mol Cancer Res **5:**1001–1014. http://dx.doi.org/10.1158/1541-7786.MCR-07-0119.
27. **Gentleman RC, Carey VJ, Bates DM, Bolstad B, Dettling M, Dudoit S, Ellis B, Gautier L, Ge Y, Gentry J, Hornik K, Hothorn T, Huber W, Iacus S, Irizarry R, Leisch F, Li C, Maechler M, Rossini AJ, Sawitzki G, Smith C, Smyth G, Tierney L, Yang JY, Zhang J.** 2004. Bioconductor: open software development for computational biology and bioinformatics. Genome Biol **5:**R80. http://dx.doi.org/10.1186/gb-2004-5-10-r80.
28. **Ouellet V, Tiedemann K, Mourskaia A, Fong JE, Tran-Thanh D, Amir E, Clemons M, Perbal B, Komarova SV, Siegel PM.** 2011. CCN3 impairs osteoblast and stimulates osteoclast differentiation to favor breast cancer metastasis to bone. Am J Pathol **178:**2377–2388. http://dx.doi.org/10.1016/j.ajpath.2011.01.033.
29. **Gyorffy B, Lanczky A, Eklund AC, Denkert C, Budczies J, Li Q, Szallasi Z.** 2010. An online survival analysis tool to rapidly assess the effect of 22,277 genes on breast cancer prognosis using microarray data of 1,809 patients. Breast Cancer Res Treat **123:**725–731. http://dx.doi.org/10.1007/s10549-009-0674-9.
30. **Gyorffy B, Lanczky A, Szallasi Z.** 2012. Implementing an online tool for genome-wide validation of survival-associated biomarkers in ovarian-cancer using microarray data from 1287 patients. Endocr Relat Cancer **19:**197–208. http://dx.doi.org/10.1530/ERC-11-0329.
31. **Gyorffy B, Surowiak P, Budczies J, Lanczky A.** 2013. Online survival analysis software to assess the prognostic value of biomarkers using transcriptomic data in non-small-cell lung cancer. PLoS One **8:**e82241. http://dx.doi.org/10.1371/journal.pone.0082241.
32. **Dickins RA, Hemann MT, Zilfou JT, Simpson DR, Ibarra I, Hannon GJ, Lowe SW.** 2005. Probing tumor phenotypes using stable and regulated synthetic microRNA precursors. Nat Genet **37:**1289–1295.
33. **Fernandes H, Dechering K, van Someren E, Steeghs I, Apotheker M, Mentink A, van Blitterswijk C, de Boer J.** 2010. Effect of chordin-like 1 on MC3T3-E1 and human mesenchymal stem cells. Cells Tissues Organs **191:**443–452. http://dx.doi.org/10.1159/000281825.
34. **Soofi A, Zhang P, Dressler GR.** 2013. Kielin/chordin-like protein attenuates both acute and chronic renal injury. J Am Soc Nephrol **24:**897–905. http://dx.doi.org/10.1681/ASN.2012070759.
35. **Wang SE, Xiang B, Guix M, Olivares MG, Parker J, Chung CH, Pandiella A, Arteaga CL.** 2008. Transforming growth factor beta engages TACE and ErbB3 to activate phosphatidylinositol-3 kinase/Akt in ErbB2-overexpressing breast cancer and desensitizes cells to trastuzumab. Mol Cell Biol **28:**5605–5620. http://dx.doi.org/10.1128/MCB.00787-08.
36. **Hoshino D, Branch KM, Weaver AM.** 2013. Signaling inputs to invadopodia and podosomes. J Cell Sci **126:**2979–2989. http://dx.doi.org/10.1242/jcs.079475.
37. **Murphy DA, Courtneidge SA.** 2011. The 'ins' and 'outs' of podosomes and invadopodia: characteristics, formation and function. Nat Rev Mol Cell Biol **12:**413–426. http://dx.doi.org/10.1038/nrm3141.
38. **Chen WT, Wang JY.** 1999. Specialized surface protrusions of invasive cells, invadopodia and lamellipodia, have differential MT1-MMP, MMP-2, and TIMP-2 localization. Ann N Y Acad Sci **878:**361–371. http://dx.doi.org/10.1111/j.1749-6632.1999.tb07695.x.
39. **Nakahara H, Howard L, Thompson EW, Sato H, Seiki M, Yeh Y, Chen WT.** 1997. Transmembrane/cytoplasmic domain-mediated membrane type 1-matrix metalloprotease docking to invadopodia is required for cell invasion. Proc Natl Acad Sci U S A **94:**7959–7964. http://dx.doi.org/10.1073/pnas.94.15.7959.
40. **Beaty BT, Wang Y, Bravo-Cordero JJ, Sharma VP, Miskolci V, Hodgson L, Condeelis J.** 2014. Talin regulates moesin-NHE-1 recruitment to invadopodia and promotes mammary tumor metastasis. J Cell Biol **205:** 737–751. http://dx.doi.org/10.1083/jcb.201312046.
41. **Coopman PJ, Do MT, Thompson EW, Mueller SC.** 1998. Phagocytosis of cross-linked gelatin matrix by human breast carcinoma cells correlates with their invasive capacity. Clin Cancer Res **4:**507–515.
42. **Rajadurai CV, Havrylov S, Zaoui K, Vaillancourt R, Stuible M, Naujokas M, Zuo D, Tremblay ML, Park M.** 2012. Met receptor tyrosine

kinase signals through a cortactin-Gab1 scaffold complex, to mediate invadopodia. J Cell Sci **125:**2940–2953. http://dx.doi.org/10.1242/jcs.100834.
43. **Deryugina EI, Ratnikov B, Monosov E, Postnova TI, DiScipio R, Smith JW, Strongin AY.** 2001. MT1-MMP initiates activation of pro-MMP-2 and integrin alphavbeta3 promotes maturation of MMP-2 in breast carcinoma cells. Exp Cell Res **263:**209–223. http://dx.doi.org/10.1006/excr.2000.5118.
44. **Sato H, Takino T, Kinoshita T, Imai K, Okada Y, Stetler Stevenson WG, Seiki M.** 1996. Cell surface binding and activation of gelatinase A induced by expression of membrane-type-1-matrix metalloproteinase (MT1-MMP). FEBS Lett **385:**238–240. http://dx.doi.org/10.1016/0014-5793(96)00389-4.
45. **Ye L, Bokobza SM, Jiang WG.** 2009. Bone morphogenetic proteins in development and progression of breast cancer and therapeutic potential (review). Int J Mol Med **24:**591–597.
46. **Rothhammer T, Bataille F, Spruss T, Eissner G, Bosserhoff AK.** 2007. Functional implication of BMP4 expression on angiogenesis in malignant melanoma. Oncogene **26:**4158–4170. http://dx.doi.org/10.1038/sj.onc.1210182.
47. **Rothhammer T, Poser I, Soncin F, Bataille F, Moser M, Bosserhoff AK.** 2005. Bone morphogenic proteins are overexpressed in malignant melanoma and promote cell invasion and migration. Cancer Res **65:**448–456.
48. **Clement JH, Raida M, Sanger J, Bicknell R, Liu J, Naumann A, Geyer A, Waldau A, Hortschansky P, Schmidt A, Hoffken K, Wolft S, Harris AL.** 2005. Bone morphogenetic protein 2 (BMP-2) induces in vitro invasion and in vivo hormone independent growth of breast carcinoma cells. Int J Oncol **27:**401–407.
49. **Jin H, Pi J, Huang X, Huang F, Shao W, Li S, Chen Y, Cai J.** 2012. BMP2 promotes migration and invasion of breast cancer cells via cytoskeletal reorganization and adhesion decrease: an AFM investigation. Appl Microbiol Biotechnol **93:**1715–1723. http://dx.doi.org/10.1007/s00253-011-3865-3.
50. **Scherberich A, Tucker RP, Degen M, Brown-Luedi M, Andres AC, Chiquet-Ehrismann R.** 2005. Tenascin-W is found in malignant mammary tumors, promotes alpha8 integrin-dependent motility and requires p38MAPK activity for BMP-2 and TNF-alpha induced expression in vitro. Oncogene **24:**1525–1532. http://dx.doi.org/10.1038/sj.onc.1208342.
51. **Braig S, Bosserhoff AK.** 2013. Death inducer-obliterator 1 (Dido1) is a BMP target gene and promotes BMP-induced melanoma progression. Oncogene **32:**837–848. http://dx.doi.org/10.1038/onc.2012.115.
52. **Moll F, Millet C, Noel D, Orsetti B, Bardin A, Katsaros D, Jorgensen C, Garcia M, Theillet C, Pujol P, Francois V.** 2006. Chordin is underexpressed in ovarian tumors and reduces tumor cell motility. FASEB J **20:**240–250. http://dx.doi.org/10.1096/fj.05-4126com.
53. **Owens P, Polikowsky H, Pickup MW, Gorska AE, Jovanovic B, Shaw AK, Novitskiy SV, Hong CC, Moses HL.** 2013. Bone morphogenetic proteins stimulate mammary fibroblasts to promote mammary carcinoma cell invasion. PLoS One **8:**e67533. http://dx.doi.org/10.1371/journal.pone.0067533.
54. **Miyazawa Y, Uekita T, Ito Y, Seiki M, Yamaguchi H, Sakai R.** 2013. CDCP1 regulates the function of MT1-MMP and invadopodia-mediated invasion of cancer cells. Mol Cancer Res **11:**628–637. http://dx.doi.org/10.1158/1541-7786.MCR-12-0544.
55. **Miura S, Hamada S, Masamune A, Satoh K, Shimosegawa T.** 2014. CUB-domain containing protein 1 represses the epithelial phenotype of pancreatic cancer cells. Exp Cell Res **321:**209–218. http://dx.doi.org/10.1016/j.yexcr.2013.12.019.
56. **Owens P, Pickup MW, Novitskiy SV, Giltnane JM, Gorska AE, Hopkins CR, Hong CC, Moses HL.** 2015. Inhibition of BMP signaling suppresses metastasis in mammary cancer. Oncogene **34:**2437–2449. http://dx.doi.org/10.1038/onc.2014.189.
57. **Gao H, Chakraborty G, Lee-Lim AP, Mo Q, Decker M, Vonica A, Shen R, Brogi E, Brivanlou AH, Giancotti FG.** 2012. The BMP inhibitor Coco reactivates breast cancer cells at lung metastatic sites. Cell **150:**764–779. http://dx.doi.org/10.1016/j.cell.2012.06.035.
58. **Tarragona M, Pavlovic M, Arnal-Estape A, Urosevic J, Morales M, Guiu M, Planet E, Gonzalez-Suarez E, Gomis RR.** 2012. Identification of NOG as a specific breast cancer bone metastasis-supporting gene. J Biol Chem **287:**21346–21355. http://dx.doi.org/10.1074/jbc.M112.355834.
59. **Cao Y, Slaney CY, Bidwell BN, Parker BS, Johnstone CN, Rautela J, Eckhardt BL, Anderson RL.** 2014. BMP4 inhibits breast cancer metastasis by blocking myeloid-derived suppressor cell activity. Cancer Res **74:**5091–5102. http://dx.doi.org/10.1158/1538-7445.AM2014-5091. http://dx.doi.org/10.1158/0008-5472.CAN-13-3171.
60. **Langenfeld EM, Bojnowski J, Perone J, Langenfeld J.** 2005. Expression of bone morphogenetic proteins in human lung carcinomas. Ann Thorac Surg **80:**1028–1032. http://dx.doi.org/10.1016/j.athoracsur.2005.03.094.
61. **Langenfeld EM, Calvano SE, Abou-Nukta F, Lowry SF, Amenta P, Langenfeld J.** 2003. The mature bone morphogenetic protein-2 is aberrantly expressed in non-small cell lung carcinomas and stimulates tumor growth of A549 cells. Carcinogenesis **24:**1445–1454. http://dx.doi.org/10.1093/carcin/bgg100.
62. **Langenfeld EM, Langenfeld J.** 2004. Bone morphogenetic protein-2 stimulates angiogenesis in developing tumors. Mol Cancer Res **2:**141–149.
63. **Laatio L, Myllynen P, Serpi R, Rysa J, Ilves M, Lappi-Blanco E, Ruskoaho H, Vahakangas K, Puistola U.** 2011. BMP-4 expression has prognostic significance in advanced serous ovarian carcinoma and is affected by cisplatin in OVCAR-3 cells. Tumour Biol **32:**985–995. http://dx.doi.org/10.1007/s13277-011-0200-7.